(Gibco, Grand Island, NY, USA) supplemented with 10% fetal bovine serum (FBS) (Sigma, St. Louis, MO, USA) and an antibiotic/antimycotic mixture (100 U/ml each) (Gibco) and were cultured in a humidified incubator (5% CO_2) at 37°C. The medium was replaced with fresh medium every 3–4 days. Prior to each experiment, the cells were seeded into 6- or 12-well plates and allowed to attach for at least 24 hr (6-well for triglyceride [TG] assay and 12-well for RNA extraction).

Transfection. Using SuperFect Transfection Reagent (Qiagen, Tokyo), cells were transfected with 4 or 3 μg of pCAG-HCVcore or pCAG-MOK (4 μg for 6-well plates and 3 μg for 12-well plates) and were cultured in DMEM with 10% FBS. After 24 or 48 hr, the cells were harvested for analysis. The efficiency of transfection was investigated using pCAG-LacZ. Cells were washed with phosphate-buffered saline (PBS) and fixed with 2% formaldehyde and 0.2% glutaraldehyde in PBS. Then the cells were stained with X-gal using a β-Gal Staining Set (Roche, Tokyo).

Animals. Adult male C57BL/6 mice (Charles River Laboratories, Yokohama, Japan), which were over 8 weeks old and weighed 21–24 g, were used in this study. All animals were housed in an environmentally controlled facility with a 12-hr lighting time (lights on from 0700 until 1900 hr). They were given free access to standard chow and water. Experiments (intravenous injection and sacrifice) were performed from 0900 to 21 hr. The animals received humane care according to the institutional guidelines for handling experimental animals.

HCV Core Protein Expression in Mice. The animals received an intravenous injection of 1×10^9 pfu (plaque-forming units) of AdexCAHCVcore or AdexCAlacZ and were sacrificed 3 days later. Mice were anesthetized with pentobarbital (100 mg/kg intraperitoneally). Blood was collected by cardiac puncture with a heparinized syringe, after which the liver was rapidly removed, weighed, and perfused with ice-cold PBS (pH 7.4). Part of the liver was fixed in 10% neutral buffered formalin and embedded in paraffin for histologic analysis. Another part was stored in RNA later reagent (Qiagen, Tokyo) at 4°C for extraction of RNA, and the remaining liver tissue was snap-frozen in liquid nitrogen and stored at −80°C until required. Plasma was immediately separated by centrifugation (10,000 rpm at 4°C) and stored at −20°C.

Liver Histology and Serum ALT Level. Sections of liver tissue (4 μm thick) were stained with hematoxylin and eosin for analysis. The serum alanine aminotransferase (ALT) level was measured using an automated technique by SRL Co. (Hiroshima, Japan).

HCV Core Protein Expression in Cells. Proteins were extracted from cells using PRO-PREP protein extraction solution (containing 1.0 mM PMSF, 1.0 mM EDTA, 1 μM pepstatin, 1 μM leupeptin, and 1 μM aprotinin) (Intron Biotechnology, Kyungki-Do, Korea). HCV core antigen levels were measured in cells using an HCV core antigen enzyme-linked immunosorbent assay (ELISA) (Ortho-Clinical Diagnostics K.K., Tokyo).

HCV Core Protein Expression in Mice. We confirmed HCV core protein expression in liver tissue by Western blot analysis. Proteins were extracted using PRO-PREP protein extraction solution. Then 50 μg of protein was separated by sodium dodecyl sulfate–polyacrylamide gel electrophoresis and transferred to a nitrocellulose membrane (Millipore, Bedford, MA, USA) using a tank blotting system according to the manufacturer's instructions (Bio-Rad Laboratories). After transfer, the membrane was blocked for 2 hr at room temperature with 5% powdered skim milk dissolved in Tris-buffered saline containing 0.05% between 20 and then incubated overnight at 4°C with a monoclonal mouse antibody to HCV core protein (kindly provided by Ortho-Clinical Diagnostics K.K.). Immune complexes were detected using alkaline phosphatase-conjugated anti-mouse IgG (Cosmo Bio, Tokyo) according to the manufacturer's instructions (Bio-Rad Laboratories). Detection of HCV core protein was performed by comparison with the following standards: myosin (200 kDa), β-galactosidase (116 kDa), bovine serum albumin (66 kDa), carbonic anhydrase (31 kDa), soybean trypsin inhibitor (21.5 kDa), lysozyme (14.4 kDa), and aprotinin (6.5 kDa).

Measurement of Triglyceride Content. After the medium was removed, the cells were washed three times with PBS and resuspended in 200 μl of PBS. Then lipids were extracted from 100 μl of PBS by the method of Bligh and Dyer (27) and resuspended in 100 μL of 10% Triton X. The cellular content of TG was measured using enzyme reagents and standards from Wako (Osaka, Japan). The remainder of the PBS suspension was used for the protein assay. In mice experiments, livers were homogenized in PBS and 100 μl of the homogenate was used for extraction of lipids. Total protein was measured with protein assay reagents from Bio-Rad (Richmond, CA, USA).

Hepatic Level of Thiobarbituric Acid-Reactive Substances (TBARS). The hepatic level of TBARS was measured using an OXI-TEK TBARS Assay Kit (Zeptometrix Corporation, New York, USA). Briefly, 100 mg of liver tissue was homogenized in 10 vol of normal saline. Then 100 μl of SDS and 2.5 ml of TBA/buffer reagent were added to 100 μl of this homogenate or the malondialdehyde standard. Samples were incubated at 95°C for 60 min, cooled in an ice bath for 10 min, and centrifuged at 3000 rpm for 15 min, after which the supernatant was analyzed by spectrophotometry (532 nm).

Extraction of RNA and RT-PCR. The medium was removed and the cells were washed twice with PBS. After centrifugation, total RNA was isolated using an RNeasy Mini Kit (Qiagen, Tokyo). From mouse, 20 mg of liver tissue was used for RNA extraction. Then 2 μg of total RNA was employed for reverse transcription using random hexamers (final concentration: 2.5 μM) and murine leukemia virus reverse transcriptase (final concentration: 2.5 U/μl) (Roche, Tokyo). Specific primer sets were synthesized for performance of the PCR (Table 1) and were used for assessment of liver-predominant mitochondrial carnitine palmitoyl transferase-1 (CPT1A in humans and CPT1 in mice; the rate-limiting enzyme of mitochondrial β-oxidation), acyl-CoA oxidase (ACO1 in humans and AOX in mice: the rate-limiting enzyme of peroxisomal β-oxidation), cytochrome P-450 4A11 (CYP4A11; involved in microsomal ω-oxidation), multidrug resistance protein 3 (MDR3 in humans and Mdr2 in mice; an ABC transporter and phospholipid flippase), microsomal TG transfer protein (MTP: a vital protein for TG incorporation into VLDL), and two nuclear receptors (peroxisome proliferator-activated receptor α[PPARα]] and peroxisome proliferator-activated receptor γ (PPARγ). Roles of these genes are summarized in Table 2. Amplification involved 30 cycles of denaturation at 95°C for 60 sec, annealing at each specified temperature (Table 1) for 30 sec, and extension at 72°C for 60 sec. The reaction products were analyzed on a 2% agarose gel and were visualized by ethidium bromide staining. The PCR products were excised from the gel, purified using a gel purification kit (Qiagen), and quantified by spectrophotometry. Dilutions

TABLE 1. PRIMER SETS IN THE EXPERIMENTS

	Forward	*Reverse*	*Annealing temp. (°C)*
Human			
GAPDH	GAACGGGAAGCTCACTGGCATGGC	TGAGGTCCACCCTGTTGCTG	65
PPARα	GGAAAGCCCACTCTGCCCCCT	AGTCACCGAGGAGGGGCTCGA	63
PPARγ	CATTCTGGCCCACCAACTTTGG	TGGAGATGCAGGCTCCACTTTG	63
MDR3 (ABCB4)	GATGAAAAGGCTGCCACTAG	TTGCACTTCTGCTGCTTCAC	62
MTP	GGCTAGCCTATTTCAGACACA	GATGAGCCTGGTAGGTCACT	60
CPT1A	AGACGGTGGAACAGAGGCTGAAG	TGAGACCAAACAAAGTGATGATGTCAG	67
ACO1	GGGCATGGCTATTCTCATTGC	CGAACAAGGTCAACAGAAGTTAGGTTC	60
CYP4A11	GTGGCCCAACCCAGAGGT	TCCCAATGCAGTTCCTTGATC	55
Mouse			
GAPDH	AGAACATCCCTGCATCC	TTGTCATTGAGAGCAATGCC	56
PPARα	TGCAGAGCAACCATCCAG	TAATGGCGAATTATAAAC	50
PPARγ	GGTGAAACTCTGGGAGATTC	CAACCATTGGGTCAGCTCTT	59
Mdr2 (Abcb4)	TATCCGCTATGGCCGTGGGAA	ATCGGTGAGCTATCACAATGG	56
MTP	TGAGCGGCTATACAAGCTCAC	CTGGAAGATGCTCTTCTCGC	60
LCPT	CGCACGGAAGGAAAATGG	TGTGCCCAATATTCCTGG	52
AOX	CTTGTTCGCGCAAGTGAGG	CAGGATCCGACTGTTTACC	56

ranging from 3×10^{-5} to 3×10^{2} pg were prepared in water and used as the standards.

Quantitative PCR. Quantitative PCR was performed using the Light-Cycler Fast-Start DNA Master SYBR Green system (Roche Molecular Biochemicals, Tokyo). PCR was carried out in a final reaction volume of 20 μl using 1 μl of each primer at 10 μM (final concentration: 0.5 μM), 1.6 μl of 25 mM $MgCl_2$(final concentration: 3 mM), 2 μl of the enzyme mix supplied, 12.4 μl of H_2O, and 2 μl of the template. The enzyme mix contained the reaction buffer, Fast-Start Taq DNA polymerase, and DNA double strand-specific SYBR Green I dye for detection of PCR products. PCR was performed in a Light-Cycler (Roche) with preincubation for 10 min at 95°C followed by 40 cycles of denaturation for 15 sec at 95°C, annealing for 5 sec at each specified temperature (see Table 1), and extension for 25 sec at 72°C, with fluorescent detection at the end of extension. Next, the PCR products were subjected to melting curve analysis to exclude the amplification of primer dimmers or other nonspecific products. If primer dimmers and nonspecific bands were detected, fluorescence detection was repeated after extension at each specified temperature for 1 sec. Analysis was carried out with Light-Cycler 3.5 software (Roche). Quantification was done using the "point fitting" mode and baseline adjustment. The standard curve for each gene was created using five different dilutions. The plot of the number of PCR cycles versus log concentration was considered reliable when the error was <0.2.

Statistical Analysis. Results are expressed as the mean ± SE. Statistical analysis was performed using Student's *t*-test, and $P < 0.05$ was defined as indicating significance.

RESULTS

HCV Core Protein Expression in HepG2 Cells. The transfection efficiency of pCAG-LacZ was about 20%. HCV core protein expression by the cells was confirmed using the HCV core antigen ELISA. No HCV core antigen was detected in mock-transfected and nontransfected cells. The level of HCV core protein expression showed no difference between 24 and 48 hr after transfection (24 hr,

TABLE 2. ROLES OF ANALYZED GENES IN FATTY ACID METABOLISM

MDR3	Multidrug resistance protein 3
	An ABC transporter and phospholipid flippase
	Role: Phospholipid secretion into bile
MTP	Microsomal triglyceride transfer protein
	A vital protein for TG incorporation into VLDL
	Role: triglyceride secretion into blood
CPT1A	Liver-predominant mitochondrial carnitine palmitoyl transferase-1
	The rate-limiting enzyme of mitochondrial β-oxidation
	Role: Fatty acid β-oxidation in the liver
ACO1	Acyl-CoA oxidase
	The rate-limiting enzyme of peroxisomal β-oxidation
	Role: Fatty acid β-oxidation in the liver
PPARα	Peroxisome proliferator-activated receptor α
	A nuclear receptor
	Role: A nuclear receptor controlling lipid metabolism-associated genes
PPARγ	Peroxisome proliferator-activated receptor γ
	A nuclear receptor
	Role: A nuclear receptor controlling lipid metabolism-associated genes

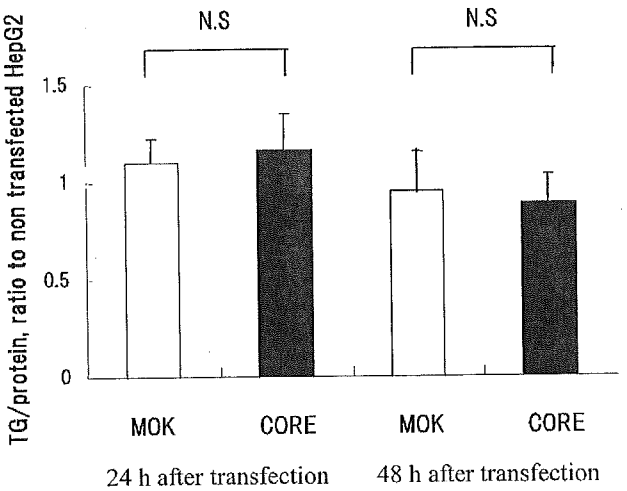

Fig 2. Effect of HCV core protein expression on cellular triglyceride (TG) content. Four micrograms of pCAG-MOK (control) or pCAG-HCVcore was transfected into HepG2 cells cultured in six-well plates by the lipofection method. At 24 or 48 hr after transfection, cells were collected for protein assay and lipid extraction. TG content was measured and expressed as the ratio to the protein content. Data are shown as values relative to those for nontransfected HepG2 cells. Each data point represents the mean ± SD of six individual experiments. P = NS compared with pCAG-MOK (Student's t-test).

1.31 ± 0.20 nmol/mg protein; 48 hr, 1.25 ± 0.16 nmol/mg protein).

TG Content of HepG2 Cells. The cellular TG content at 24 hr after transfection showed no difference between HCV core transfectants (CORE) and mock transfectants (MOK) as control (CORE, 1.16 ± 0.19; MOK, 1.10 ± 0.13; $P = 0.57$). At 48 hr after transfection, the TG content also showed no difference between the groups (CORE, 0.88 ± 0.16; MOK, 0.95 ± 0.18; $P = 0.55$). Data are expressed as the ratio to nontransfected cells (Figure 2).

Expression of Target Genes by HepG2 Cells. At 24 hr after transfection, HCV CORE showed increased expression of mRNA for PPAR γ (CORE, 2.39 ± 0.26; MOK, 1.98 ± 0.28; $P = 0.025$), MDR3 (CORE, 1.30 ± 0.21; MOK, 1.02 ± 0.20; $P = 0.030$), MTP (CORE, 0.37 ± 0.04; MOK, 0.26 ± 0.05; $P < 0.01$), and ACO1 (CORE, 1.11 ± 0.14; MOK, 0.76 ± 0.08; $P < 0.01$)gompared to MOK, while CPT (CORE, 1.18 ± 0.16; MOK, 0.94 ± 0.28; $P = 0.102$) and PPARα (CORE, 0.84 ± 0.14; MOK, 0.69 ± 0.10; $P = 0.055$) expression was normal (Figure 3). At 48 hr after transfection, HCV CORE showed lower expression of mRNA for PPAR α (CORE, 0.89 ± 0.02; MOK, 0.96 ± 0.08;

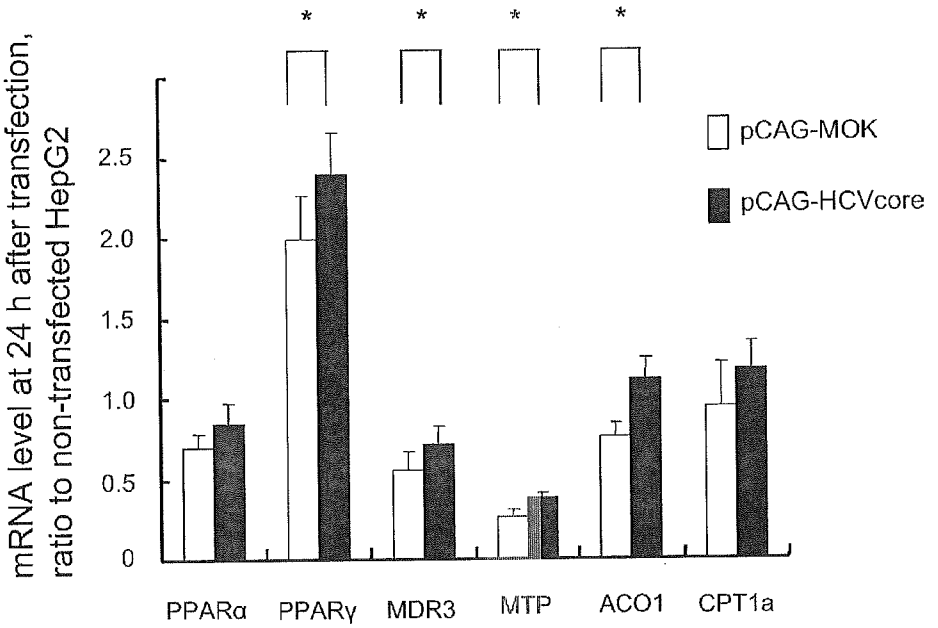

Fig 3. Effect of HCV core protein expression on mRNA levels at 24 hr after transfection. Three micrograms of pCAG-MOK (control) or pCAG-HCVcore was transfected into HepG2 cells cultured in 12-well plates by the lipofection method. At 24 hr after transfection, cells were collected for extraction of RNA. Complementary DNA was synthesized from 2 μg of RNA and used for quantified PCR with the Light-Cycler Fast-Start DNA Master SYBR Green system. GAPDH level was measured as the internal control, and the ratio to GAPDH was calculated for each sample. Data are shown as values relative to those for nontransfected HepG2 cells. Each data point represents the mean ± SD of 6 individual experiments. *$P < 0.05$ compared with pCAG-MOK (Student's t-test).

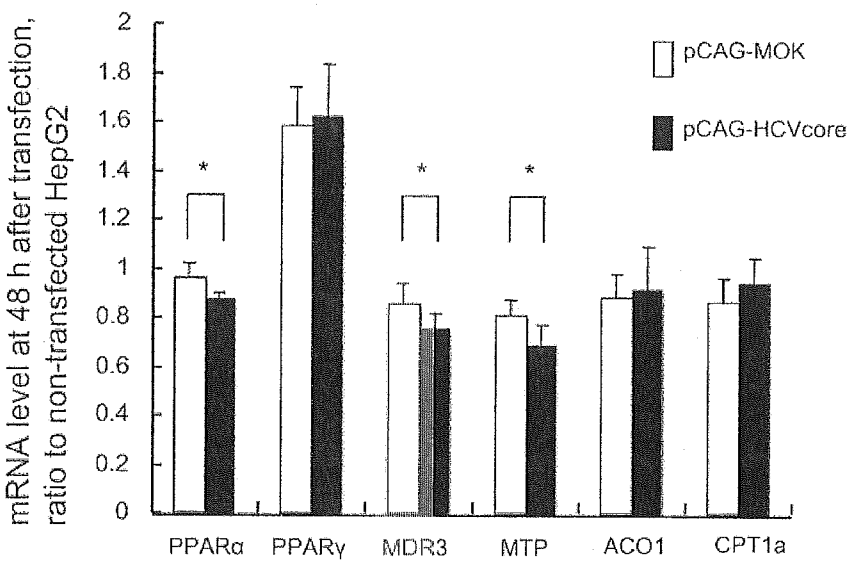

Fig 4. Effect of HCV core protein on mRNA expression at 48 hr after transfection. Three micrograms of pCAG-MOK (control) or pCAG-HCVcore was transfected into HepG2 cells cultured in 12-well plates by the lipofection method. At 48 hr after transfection, cells were collected and used for RNA extraction. Complementary DNA was synthesized from 2 μg of RNA and used for quantified PCR with the Light-Cycler Fast-Start DNA Master SYBR Green system. GAPDH was measured as an internal control, and the ratio to GAPDH was calculated for each sample. Data are shown as values relative to those for nontransfected HepG2 cells. Each data point represents the mean ± SD of 6 individual experiments. * $P < 0.05$ compared with pCAG-MOK (Student's t-test).

$P = 0.048$), MDR3 (CORE, 0.75 ± 0.06; MOK, 0.86 ± 0.08; $P = 0.031$), and MTP (CORE, 0.69 ± 0.08; MOK, 0.81 ± 0.07; $P = 0.016$) compared with MOK, while ACO1 returned to the control level (CORE, 0.91 ± 0.18; MOK, 0.88 ± 0.09; $P = 0.70$) and the CPT level was normal (CORE, 0.94 ± 0.13; MOK, 0.86 ± 0.10; $P = 0.27$). Data are expressed as the ratio to nontransfected cells (Figure 4). Experiments were repeated three times and similar results were obtained, with statistical significance. CYP4A11 was not detected by RT-PCR, so we could not make a standard for the Light-Cycler.

HCV Core Protein Expression in Mice. HCV core protein-expressing mice looked healthy and their body weight (BW) and liver weight remained within the normal range (BW [g]: PBS, 22.5 ± 0.816; AdexCAHCVcore (CORE), 21.7 ± 0.84; AdexCAlacZ (LacZ), as control, 21.5 ± 0.71). Similar mild elevation of ALT and mild hepatic lymphocyte infiltration were observed in both groups of adenovirus-infected mice, showing no differences between Core and LacZ (GPT [IU/ml]: PBS, 65 ± 17.8; CORE, 170 ± 59.4; LacZ, 142.5 ± 82.2). Lipid drops were not observed in either group (data not shown). Western blot analysis revealed the HCV core protein of about 19–20 kDa (Figure 5). In preliminary experiments, animals receiving an intravenous injection of 1×10^9 pfu developed severe hepatitis after 7 days, while animals receiving 1×10^8 pfu showed amild elevation of ALT, but their HCV core protein expression (based on quantification of mRNA and HCV core antigen) was significantly lower at 7 days after injection. Thus, we selected injection of 1×10^9 pfu and sacrifice at 3 days for the study protocol.

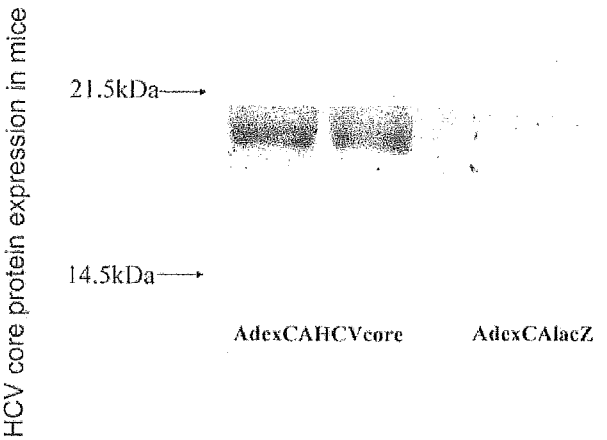

Fig 5. HCV core protein expression in mice. AdexCAlacZ (control recombinant adenovirus) or AdexCAHCVcore was used to infect male C57BL/6 mice (8–10 weeks old) by intravenous administration (1×10^9 pfu). Three days after infection, livers were collected for protein assay. Using 50 μg of protein, HCV core protein expression was confirmed by Western blotting with a mouse monoclonal antibody for HCV core protein (19–20 kDa).

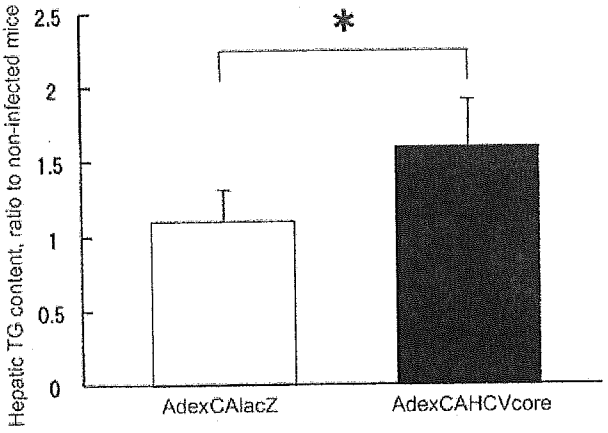

Fig 6. Effect of HCV core protein expression on the hepatic triglyceride content in mice. AdexCAlacZ (control adenovirus) or AdexCAHCVcore was used to infect male C57BL/6 mice (8–10 weeks old) by intravenous administration (1×10^9 pfu). At 3 days after infection, the livers were collected and 100 μl of liver homogenate was used for lipid extraction and for the protein assay. The TG content was measured and expressed as the ratio to the protein content. Data are shown as values relative to those for noninfected mice. Each data point represents the mean ± SD of four individual mice. $^*P < 0.05$ compared with AdexCAlacZ (control adenovirus) by Student's t-test.

Hepatic TG Level in Mice. Animals injected with AdexCAHCVcore showed a 1.45-fold increase in hepatic TG content compared to animals injected with AdexCAlacZ (CORE, 1.60 ± 0.33; LacZ, 1.10 ± 0.21; $P = 0.044$; $N = 4$). Data are expressed as the ratio to noninfected mice (Figure 6).

Expression of Target Genes in Mice. In the livers of HCV core protein-expressing mice, PPAR α (CORE, 0.59 ± 0.11; LacZ, 1.33 ± 0.21; $P < 0.01$), PPAR γ (CORE, 1.05 ± 0.10; LacZ, 2.43 ± 0.69; $P < 0.01$), Mdr2 (CORE, 0.85 ± 0.08; LacZ, 1.12 ± 0.12; $P = 0.011$), AOX (CORE, 0.235 ± 0.08; LacZ, 0.401 ± 0.07; $P = 0.02$), and CPT (CORE, 1.14 ± 0.14; LacZ 2.34 ± 0.51; $P < 0.01$) were all down-regulated, while the level of MTP mRNA was unchanged (CORE, 1.37 ± 0.08; LacZ, 1.24 ± 0.17; $P = 0.22$; $N = 4$). Data are expressed as the ratio to noninfected mice (Figure 7).

Hepatic TBARS Level. In the livers of HCV core protein-expressing mice, the TBARS level was increased compared with that in the control group (CORE, 0.84 ± 0.08; LacZ, 0.41 ± 0.01; $P < 0.01$; $N = 4$) (Figure 8).

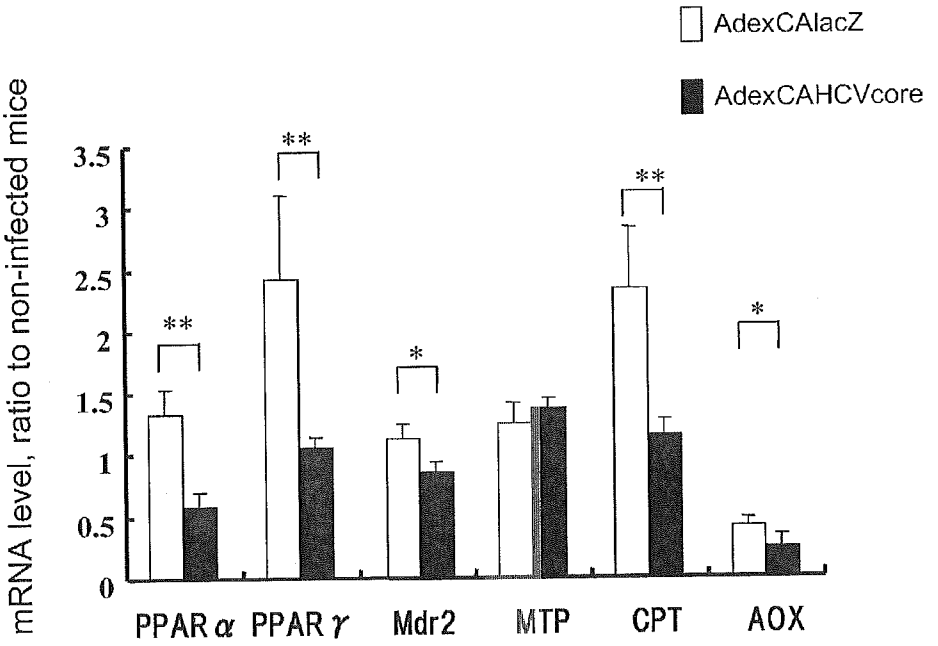

Fig 7. Effect of HCV core protein expression on mRNA levels in mice. AdexCAlacZ (control adenovirus) or AdexCAHCVcore was used to infect male C57BL/6 mice (8–10 weeks old) by intravenous administration (1×10^9 pfu). At 3 days after infection, livers were collected for RNA extraction. Complementary DNA was synthesized from 2 μg of RNA and used for quantified PCR with the Light-Cycler Fast-Start DNA Master SYBR Green system. GAPDH was measured as an internal control, and the ratio to GAPDH was calculated for each sample. Data are shown as relative values to those for noninfected mice. Each data point represents the mean ± SD of four individual mice. $^*P < 0.05$ and $^{**}P < 0.01$ compared with AdexCAlacZ (control adenovirus) by Student's t-test.

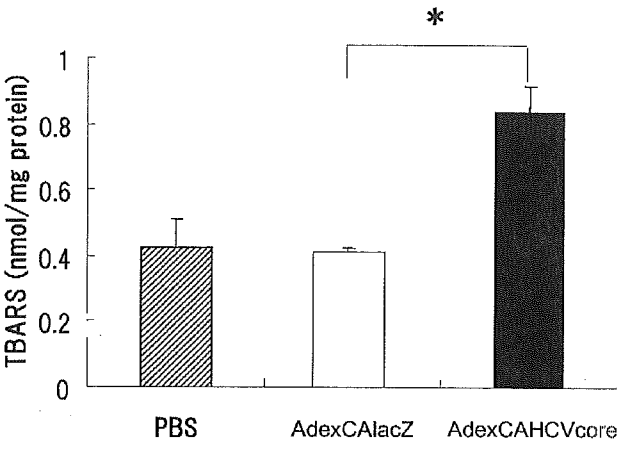

Fig 8. Effect of HCV core protein expression on TBARS in the mouse liver. AdexCAlacZ (control adenovirus) or AdexCAHCVcore was used to infect male C57BL/6 mice (8–10 weeks old) by intravenous administration (1×10^9 pfu). At 3 days after infection, livers were homogenized in 10 vol of normal saline. TBARS and total protein (TP) levels were measured as described under Materials and Methods. Data are expressed as the ratio to the TP level. Each data point represents the mean ± SD of four individual mice. $^*P < 0.01$ compared with AdexCAlacZ (control adenovirus) by Student's t-test.

DISCUSSION

HCV core protein was recently reported to cause hepatic steatosis and induction of reactive oxygen species (ROS) in an HCV core protein transgenic mouse model (18–20). In the transgenic mouse model, it was also shown that a decrease in MTP activity contributes to HCV core protein-related steatosis, while β-oxidation is unchanged (24), but the mechanism involved is still unclear. This study was the first investigation of the effect of HCV core protein on the expression of fatty acid metabolism-associated molecules in the acute expression mice model.

Hepatic accumulation of TG is principally driven by the following factors: (a) fatty acid overload (28, 29), (b) inhibition of fatty acid β-oxidation (28, 29), (c) decreased secretion of TG-rich very low density lipoprotein (VLDL) (28, 29), (d) increased de novo fatty acid synthesis, (e) decreased transformation to phospholipids, and (f) a combination of these mechanisms.

In the present study, we initially tested the effect of HCV core protein on a human cell line (HepG2). At 24 hr after transfection, the cellular TG level was unchanged, but the expression of several genes that are thought to promote fatty acid consumption (MTP, ACO1, and MDR3) was up-regulated. At 48 hr after transfection, there was either normal gene expression (ACO1) or a decrease in expression (PPARα, MDR3, and MTP). At 48 hr after transfection, the level of HCV core antigen was still the same as at 24 hr, so it seems possible that HCV core protein may act to down-regulate these genes over a longer period. To further evaluate the effects of HCV core protein, we performed in vivo experiments using transient expression of HCV core protein in mice. Although fatty change of the liver was not seen histologically, the hepatic TG level was increased by transient HCV core protein expression. In addition, expression of mRNA for all of the molecules investigated, except MTP, was down-regulated by HCV core protein expression. The mechanism involved is not understood at present, but reduced expression of these genes might contribute to hepatic TG accumulation.

CPT is the rate-limiting enzyme for mitochondrial β-oxidation (30), which is the main pathway of fatty acid consumption and ROS production. There was a recent report (20) that localization of HCV core protein in the mitochondria led to the increased production of ROS, decreased mitochondrial membrane permeability, and impairment of mitochondrial function. It remains unclear whether ROS induces fat accumulation or whether the accumulation of fat causes an increase in ROS, as well as whether decreased expression of CPT-1 is the first response to HCV core protein expression or follows other earlier changes. However, HCV core expression seems to contribute to hepatic accumulation of lipids and an increase in ROS in mice, along with reduced expression of various fatty acid metabolism-associated genes. AOX is vital for peroxisomal β-oxidation (30) and it has been reported that AOX knockout mice develop steatohepatitis, up-regulation of CYP4A gene expression, and increased production of ROS (31). We were unable to evaluate CYP4A11 in the present study, but the association of HCV-related steatosis with microsomal ω-oxidation is interesting. Mdr2 (Abcb4) is a member of the Abcb subfamily of adenosine triphosphate-binding cassette (ABC) transporter proteins. Mdr2 Pgp is exclusively localized to the canalicular membrane and controls the secretion of phospholipids into the bile (32). We thought that impaired biliary phospholipid secretion might have a role in HCV-related steatosis, based on the fact that phospholipid-associated fatty acid secretion into bile (about 25 μmol per day) is substantial in relation to the hepatic amount of triglyceride-associated fatty acids (about 75 μmol) (33). We found that the expression of MDR3 and Mdr2 was down-regulated, suggesting that reduced expression of these genes could have a causative role in HCV-related steatosis.

Interestingly, down-regulation of Mdr2, AOX, and CPT in the mice was accompanied by down-regulation of PPARα. In mice, the other three genes are thought to undergo transcriptional regulation by PPARα (33, 34), so their expression might be down-regulated secondary to the down-regulation of PPARα. HCV core protein is mainly

localized in the cytosol, but also exists in the nucleus (35, 36), so it is possible that this protein could influence gene transcription. Tsustumi *et al.* (37) used a luciferase assay to show that transcriptional activation of ACO-1 via PPRE is promoted at 24 hr after HCV core protein expression (23). However, we found down-regulation of target gene expression accompanied by decreased PPARα expression after 3 days of HCV core protein expression in mice, as well as at 48 hr after transfection of cells. The expression of PPARα was reported to be under transcriptional regulation by glucocorticoids (38), but the mechanism remains unclear. Accordingly, the mechanism leading to down-regulation of PPARα after HCV core protein expression is also unclear. The lower expression of PPARα and the genes it regulates in human hepatocytes than in mouse hepatocytes (39) could be a reason for the lack of an increase in TG and the small decline in gene expression in our cell experiment. Fibrates that bind with PPARα and increase its activity (although not its expression) might be useful for controlling HCV-related steatosis by increasing the β-oxidation and bliary secretion of fatty acids.

PPARγ improves insulin resistance and is also reported to improve hepatic fibrosis and nonalcholic steatohepatitis (40, 41). Because PPARγ gene expression also showed down-regulation by HCV core protein expression in this study , it may be necessary to examine the role of glucose metabolism, de novo synthesis of fatty acids from glucose, and fatty acid flux through hepatocytes in HCV-related steatosis.

In this study, the increase in TBARS level was found in mice with transient expression of HCV core protein. This suggests that ROS production might be induced by HCV core protein expression, although no mechanistic information for this was provided in this study. It also remains unclear whether intrahepatic fat accumulation enhances ROS production as reflected by an increase in TBARS or, inversely, whether ROS production induces fatty liver change through ROS-associated mitochondrial dysfunction. Certainly, further investigations are needed to clarify this uncertainty, but the fact that HCV core protein expression in mice contributes to the increase in TBARS level may partially characterize the pathogenesis of HCV-related hepatic damage.

In summary, transient expression of HCV core protein in mice down-regulated the expression of various lipid metabolism-associated genes (Mdr2, CPT, and AOX). It also caused down-regulation of PPARα expression and led to the accumulation of TG and the induction of oxidative stress. These findings may provide some clues to the understanding of HCV-related steatosis and to the induction of ROS production and carcinogenesis by infection with this virus.

REFERENCES

1. Alter MJ, Margolis HS, Krawczynski K, Judson FN, Mares A, Alexander WJ, Hu PY, Miller JK, Gerber MA, Sampliner RE, Meeks EL, Beach MJ: The natural history of community-acquired hepatitis C in the United States. N Engl J Med 327:1899–1905,1992
2. Seeff LB, Buskell–Bales Z, Wright EC, Durako SJ, Alter HJ, Iber FL, Hollinger FB, Gitnick G, Knodell RG, Perrillo RP, Steevens CE, Hollingworth CG, NHLBI study Group: Long-term mortality after transfusion-associated non-A, non-B hepatitis. N Engl J Med 327:1906–1911, 1992
3. Seeff LB: Natural history of hepatitis C. Hepatology 26:21S–28S, 1997
4. Koziel MJ, Dudley D, Wong JT, Dienstag J, Houghton M, Ralston R, Walker BD: Intrahepatic cytotoxic T lymphocytes specific for hepatitis C virus in persons with chronic hepatitis. J Immunol 149:3339–3344, 1992
5. Cerny A, Chisari FV: Pathogenesis of chronic hepatitis C: immunological features of hepatic injury and viral persistence. Hepatology 30:595–601, 1999
6. Rubbia-Brandt L, Quadri R, Abid K, Giostra E, Male PJ, Mentha G, Spahr L, Zarski JP, Borisch B, Hadengue A, Negro F: Hepatocyte steatosis is a cytopathic effect of hepatitis C virus genotype 3. J Hepatol 33:106–115, 2000
7. Scheuer PJ, Davies SE, Dhillon AP: Histopathological aspects of viral hepatitis. J Viral Hepat 3:277–283, 1996
8. Fujie H, Yotsuyanagi H, Moriya K, Shintani Y, Tsutsumi T, Takayama T, Makuuchi M, Matsuura Y, Miyamura T, Kimura S, Koike K: Steatosis and intrahepatic hepatitis C virus in chronic hepatitis. J Med Virol 59:141–145, 1999
9. Goodman ZD, Ishak KG: Histopathologic findings in chronic hepatitis C virus infection. Semin Liver Dis 15:70–81, 1995
10. Barba G, Harper F, Harada T, Kohara M, Goulinet S, Matsuura Y, Eder G, Schaff Z, Chapman MJ, Miyamura T, Brechot C: Hepatitis C virus core protein shows a cytoplasmic localization and associates to cellular lipid storage droplets. Proc Natl Acad Sci USA 94:1200–1205, 1997
11. Ray RB, Lagging LM, Meyer K, Ray R: Hepatitis C virus core protein cooperates with ras and transforms primary rat embryo fibroblasts to tumorigenic phenotype. J Virol 70:4438–4443, 1996
12. Ray RB, Meyer K, Ray R: Suppression of apoptotic cell death by hepatitis C virus core protein. Virology 226:176–182, 1996
13. Zhu N, Khoshnan A, Schneider R, Matsumoto M, Dennert G, Ware C, Lai MM: Hepatitis C virus core protein binds to the cytoplasmic domain of tumor necrosis factor (TNF) receptor 1 and enhances TNF-induced apoptosis. J Virol 72:3691–3697, 1998
14. Honda M, Kaneko S, Shimazaki T, Matsushita E, Kobayashi K, Ping LH, Zhang HC, Lemon SM: Hepatitis C virus core protein induces apoptosis and impairs cell-cycle regulation in stably transformed Chinese hamster ovary cells. Hepatology 31:1351–1359, 2000
15. Sakamuro D, Furukawa T, Takegami T. Sakamuro D, Furukawa T, Takegami T: Hepatitis C virus nonstructural protein NS3 transforms NIH 3T3 cells. J Virol 69:3893–3896, 1995
16. McLauchlan J, Lemberg MK, Hope G, Martoglio B: Intramembrane proteolysis promotes trafficking of hepatitis C virus core protein to lipid droplets. EMBO J 21:3980–3988, 2002
17. Shi ST, Polyak SJ, Tu H, Taylor DR, Gretch DR, Lai MM: Hepatitis C virus NS5A colocalizes with the core protein on lipid droplets and interacts with apolipoproteins. Virology 292:198–210, 2002
18. Moriya K, Yotsuyanagi H, Shintani Y, Fujie H, Ishibashi K, Matsuura Y, Miyamura T, Koike K: Hepatitis C virus core protein

induces hepatic steatosis in transgenic mice. J Gen Virol 78:1527–1531, 1997
19. Lerat H, Honda M, Beard MR, Loesch K, Sun J, Yang Y, Okuda M, Gosert R, Xiao SY, Weinman SA, Lemon SM: Steatosis and liver cancer in transgenic mice expressing the structural and nonstructural proteins of hepatitis C virus. Gastroenterology 122:352–365, 2002
20. Okuda M, Li K, Beard MR, Showalter LA, Scholle F, Lemon SM, Weinman SA: Mitochondrial injury, oxidative stress, and antioxidant gene expression are induced by hepatitis C virus core protein. Gastroenterology 122:366–375, 2002
21. Moriya K, Nakagawa K, Santa T, Shintani Y, Fujie H, Miyoshi H, Tsutsumi T, Miyazawa T, Ishibashi K, Horie T, Imai K, Todoroki T, Kimura S, Koike K: Oxidative stress in the absence of inflammation in a mouse model for hepatitis C virus-associated hepatocarcinogenesis. Cancer Res 61:4365–4370, 2001
22. Moriya K, Fujie H, Shintani Y, Yotsuyanagi H, Tsutsumi T, Ishibashi K, Matsuura Y, Kimura S, Miyamura T, Koike K: The core protein of hepatitis C virus induces hepatocellular carcinoma in transgenic mice. Nat Med 4:1065–1067, 1998
23. Sabile A, Perlemuter G, Bono F, Kohara K, Demaugre F, Kohara M, Matsuura Y, Miyamura T, Brechot C, Barba G: Hepatitis C virus core protein binds to apolipoprotein AII and its secretion is modulated by fibrates. Hepatology 30:1064–1076, 1999
24. Perlemuter G, Sabile A, Letteron P, Vona G, Topilco A, Chretien Y, Koike K, Pessayre D, Chapman J, Barba G, Brechot C: Hepatitis C virus core protein inhibits microsomal triglyceride transfer protein activity and very low density lipoprotein secretion: a model of viral-related steatosis. FASEB J 16:185–194, 2002
25. Miyake S, Makimura M, Kanegae Y, Harada S, Sato Y, Takamori K, Tokuda C, Saito I: Efficient generation of recombinant adenoviruses using adenovirus DNA-terminal protein complex and a cosmid bearing the full–length virus genome. Proc Natl Acad Sci USA 93:1320–1324, 1996
26. Kanegae Y, Lee G, Sato Y, Tanaka M, Nakai M, Sakaki T, Sugano S, Saito I: Efficient gene activation in mammalian cells by using recombinant adenovirus expressing site-specific Cre recombinase. Nucleic Acids Res 23:3816–3821, 1995
27. Bligh EG, Dyer WJ: A rapid method of total lipid extraction and purification. Can J Med Sci 37:911–917, 1959
28. Day CP, James OF: Hepatic steatosis: Innocent bystander or guilty party? Hepatology 27:1463–1466, 1988
29. Fong DG., Nehra V, Lindor KD, Buchman AL: Metabolic and nutritional considerations in nonalcoholic fatty liver. Hepatology 32:3–10, 2000
30. Reddy JK: Nonalcoholic steatosis and steatohepatitis. III. Peroxisomal beta-oxidation, PPAR alpha, and steatohepatitis. Am J Physiol Gastrointest Liver Physiol. 281:G1333–G1339, 2001 (review)
31. Fan C, Pan J, Chu R, Lee D, Kluckman KD, Usuda N, Singh I, *et al.*: Hepatocellular and hepatic peroxisomal alternation in mice with a disrupted peroxisomal fatty acyl–coenzyme A oxidase gene. J Biol Chem 271:24698–24710, 1996
32. Smit JJ, Schinkel AH: Homozygous disruption of the murine mdr2 P-glycoprotein gene leads to a complete absense of phospholipid from bile and to liver desease. Cell 75:451–462, 1993
33. Kok T, Wolters H, Bloks V, Havinga R, Jansen P, Ataels B, Kuipers F: Induction of hepatic ABC transporter expression is part of the PPARα-mediated fasting response in the mouse. Gastroenterology 124:160–171, 2002
34. Duplus E, Forest C: Is there a single mechanism for fatty acid regulation of gene transcription? Biochem Pharmacol 64:893–901, 2002 (review)
35. Moriya K, Fujie H, Shintani Y, Yotsuyanagi H, Tsutsumi T, Ishibashi K, Matsuura Y, Kimura S, Miyamura T, Koike K: The core protein of hepatitis C virus induces hepatocellular carcinoma in transgenic mouse. Nat Med 4:1065–1067, 1998
36. Yasui K: The native form and maturation process of hepatitis C virus core protein. J Virol 72:6048–6055, 1998
37. Tsutsumi T, Suzuki T, Shimoike T, Suzuki R, Moriya K, Shintani Y, Fujii H, Matsuura Y, Koike K, Miyamura T: Interaction of hepatitis C virus core protein with retinoid X receptor α modulates its transcriptional activity. Hepatology 35:937–946, 2002
38. Lemberger T, Saladin R, Vazquez M, Assimacopoulos F, Staels B, Desvergne B, Wahli W, Auwerx J: Expression of the peroxisome proliferators-activated receptor alpha gene is stimulated by stress and follows a diurnal rhythm. J Biol Chem. 19:1764–1769, 1996
39. Hsu M, Savas U, Griffin K, Johnson E: Identification of peroxisome proliferators-responsive human genes by elevated expression of peroxisome proliferators-activated receptor α in HepG2 Cells. J. Biol. Chem 276:27950–27958, 2001
40. Neuschwander-Tetri BA, Brunt EM, Wehmeier KR, Oliver D, Bacon BR: Improved nonalcoholic steatohepatitis after 48 weeks of treatment with the PPAR-gamma ligand rosiglitazone. Hepatology 38:1008–1017, 2003
41. Alter MJ, Margolis HS, Krawczynski K, Judson FN, Mares A, Alexander WJ, Hu PY, Miller JK, Gerber MA, Sampliner RE, Meeks EL, Beach MJ: The natural history of community-acquired hepatitis C in the United States. N Engl J Med 327:1899–1905,1992
42. Seeff LB, Buskell–Bales Z, Wright EC, Durako SJ, Alter HJ, Iber FL, Hollinger FB, Gitnick G, Knodell RG, Perrillo RP, Steevens CE, Hollingworth CG, NHLBI study Group: Long-term mortality after transfusion-associated non-A, non-B hepatitis. N Engl J Med 327:1906–1911, 1992
43. Seeff LB: Natural history of hepatitis C. Hepatology 26:21S–28S, 1997
44. Koziel MJ, Dudley D, Wong JT, Dienstag J, Houghton M, Ralston R, Walker BD: Intrahepatic cytotoxic T lymphocytes specific for hepatitis C virus in persons with chronic hepatitis. J Immunol 149:3339–3344, 1992
45. Cerny A, Chisari FV: Pathogenesis of chronic hepatitis C: immunological features of hepatic injury and viral persistence. Hepatology 30:595–601, 1999
46. Rubbia-Brandt L, Quadri R, Abid K, Giostra E, Male PJ, Mentha G, Spahr L, Zarski JP, Borisch B, Hadengue A, Negro F: Hepatocyte steatosis is a cytopathic effect of hepatitis C virus genotype 3. J Hepatol 33:106–115, 2000
47. Scheuer PJ, Davies SE, Dhillon AP: Histopathological aspects of viral hepatitis. J Viral Hepat 3:277–283, 1996
48. Fujie H, Yotsuyanagi H, Moriya K, Shintani Y, Tsutsumi T, Takayama T, Makuuchi M, Matsuura Y, Miyamura T, Kimura S, Koike K: Steatosis and intrahepatic hepatitis C virus in chronic hepatitis. J Med Virol 59:141–145, 1999
49. Goodman ZD, Ishak KG: Histopathologic findings in chronic hepatitis C virus infection. Semin Liver Dis 15:70–81, 1995
50. Barba G, Harper F, Harada T, Kohara M, Goulinet S, Matsuura Y, Eder G, Schaff Z, Chapman MJ, Miyamura T, Brechot C: Hepatitis C virus core protein shows a cytoplasmic localization and associates to cellular lipid storage droplets. Proc Natl Acad Sci USA 94:1200–1205, 1997
51. Ray RB, Lagging LM, Meyer K, Ray R: Hepatitis C virus core protein cooperates with ras and transforms primary rat embryo fibroblasts to tumorigenic phenotype. J Virol 70:4438–4443, 1996
52. Ray RB, Meyer K, Ray R: Suppression of apoptotic cell death by hepatitis C virus core protein. Virology 226:176–182, 1996

53. Zhu N, Khoshnan A, Schneider R, Matsumoto M, Dennert G, Ware C, Lai MM: Hepatitis C virus core protein binds to the cytoplasmic domain of tumor necrosis factor (TNF) receptor 1 and enhances TNF-induced apoptosis. J Virol 72:3691–3697, 1998
54. Honda M, Kaneko S, Shimazaki T, Matsushita E, Kobayashi K, Ping LH, Zhang HC, Lemon SM: Hepatitis C virus core protein induces apoptosis and impairs cell-cycle regulation in stably transformed Chinese hamster ovary cells. Hepatology 31:1351–1359, 2000
55. Sakamuro D, Furukawa T, Takegami T. Sakamuro D, Furukawa T, Takegami T: Hepatitis C virus nonstructural protein NS3 transforms NIH 3T3 cells. J Virol 69:3893–3896, 1995
56. McLauchlan J, Lemberg MK, Hope G, Martoglio B: Intramembrane proteolysis promotes trafficking of hepatitis C virus core protein to lipid droplets. EMBO J 21:3980–3988, 2002
57. Shi ST, Polyak SJ, Tu H, Taylor DR, Gretch DR, Lai MM: Hepatitis C virus NS5A colocalizes with the core protein on lipid droplets and interacts with apolipoproteins. Virology 292:198–210, 2002
58. Moriya K, Yotsuyanagi H, Shintani Y, Fujie H, Ishibashi K, Matsuura Y, Miyamura T, Koike K: Hepatitis C virus core protein induces hepatic steatosis in transgenic mice. J Gen Virol 78:1527–1531, 1997
59. Lerat H, Honda M, Beard MR, Loesch K, Sun J, Yang Y, Okuda M, Gosert R, Xiao SY, Weinman SA, Lemon SM: Steatosis and liver cancer in transgenic mice expressing the structural and nonstructural proteins of hepatitis C virus. Gastroenterology 122:352–365, 2002
60. Okuda M, Li K, Beard MR, Showalter LA, Scholle F, Lemon SM, Weinman SA: Mitochondrial injury, oxidative stress, and antioxidant gene expression are induced by hepatitis C virus core protein. Gastroenterology 122:366–375, 2002
61. Moriya K, Nakagawa K, Santa T, Shintani Y, Fujie H, Miyoshi H, Tsutsumi T, Miyazawa T, Ishibashi K, Horie T, Imai K, Todoroki T, Kimura S, Koike K: Oxidative stress in the absence of inflammation in a mouse model for hepatitis C virus-associated hepatocarcinogenesis. Cancer Res 61:4365–4370, 2001
62. Moriya K, Fujie H, Shintani Y, Yotsuyanagi H, Tsutsumi T, Ishibashi K, Matsuura Y, Kimura S, Miyamura T, Koike K: The core protein of hepatitis C virus induces hepatocellular carcinoma in transgenic mice. Nat Med 4:1065–1067, 1998
63. Sabile A, Perlemuter G, Bono F, Kohara K, Demaugre F, Kohara M, Matsuura Y, Miyamura T, Brechot C, Barba G: Hepatitis C virus core protein binds to apolipoprotein AII and its secretion is modulated by fibrates. Hepatology 30:1064–1076, 1999
64. Perlemuter G, Sabile A, Letteron P, Vona G, Topilco A, Chretien Y, Koike K, Pessayre D, Chapman J, Barba G, Brechot C: Hepatitis C virus core protein inhibits microsomal triglyceride transfer protein activity and very low density lipoprotein secretion: a model of viral-related steatosis. FASEB J 16:185–194, 2002
65. Miyake S, Makimura M, Kanegae Y, Harada S, Sato Y, Takamori K, Tokuda C, Saito I: Efficient generation of recombinant adenoviruses using adenovirus DNA-terminal protein complex and a cosmid bearing the full–length virus genome. Proc Natl Acad Sci USA 93:1320–1324, 1996
66. Kanegae Y, Lee G, Sato Y, Tanaka M, Nakai M, Sakaki T, Sugano S, Saito I: Efficient gene activation in mammalian cells by using recombinant adenovirus expressing site-specific Cre recombinase. Nucleic Acids Res 23:3816–3821, 1995
67. Bligh EG, Dyer WJ: A rapid method of total lipid extraction and purification. Can J Med Sci 37:911–917, 1959
68. Day CP, James OF: Hepatic steatosis: Innocent bystander or guilty party? Hepatology 27:1463–1466, 1988
69. Fong DG., Nehra V, Lindor KD, Buchman AL: Metabolic and nutritional considerations in nonalcoholic fatty liver. Hepatology 32:3–10, 2000
70. Reddy JK: Nonalcoholic steatosis and steatohepatitis. III. Peroxisomal beta-oxidation, PPAR alpha, and steatohepatitis. Am J Physiol Gastrointest Liver Physiol. 281:G1333–G1339, 2001 (review)
71. Fan C, Pan J, Chu R, Lee D, Kluckman KD, Usuda N, Singh I, *et al.*: Hepatocellular and hepatic peroxisomal alternation in mice with a disrupted peroxisomal fatty acyl–coenzyme A oxidase gene. J Biol Chem 271:24698–24710, 1996
72. Smit JJ, Schinkel AH: Homozygous disruption of the murine mdr2 P-glycoprotein gene leads to a complete absense of phospholipid from bile and to liver desease. Cell 75:451–462, 1993
73. Kok T, Wolters H, Bloks V, Havinga R, Jansen P, Ataels B, Kuipers F: Induction of hepatic ABC transporter expression is part of the PPARα-mediated fasting response in the mouse. Gastroenterology 124:160–171, 2002
74. Duplus E, Forest C: Is there a single mechanism for fatty acid regulation of gene transcription? Biochem Pharmacol 64:893–901, 2002 (review)
75. Moriya K, Fujie H, Shintani Y, Yotsuyanagi H, Tsutsumi T, Ishibashi K, Matsuura Y, Kimura S, Miyamura T, Koike K: The core protein of hepatitis C virus induces hepatocellular carcinoma in transgenic mouse. Nat Med 4:1065–1067, 1998
76. Yasui.K: The native form and maturation process of hepatitis C virus core protein. J Virol 72:6048–6055, 1998
77. Tsutsumi T, Suzuki T, Shimoike T, Suzuki R, Moriya K, Shintani Y, Fujii H, Matsuura Y, Koike K, Miyamura T: Interaction of hepatitis C virus core protein with retinoid X receptor α modulates its transcriptional activity. Hepatology 35:937–946, 2002
78. Lemberger T, Saladin R, Vazquez M, Assimacopoulos F, Staels B, Desvergne B, Wahli W, Auwerx J: Expression of the peroxisome proliferators-activated receptor alpha gene is stimulated by stress and follows a diurnal rhythm. J Biol Chem. 19:1764–1769, 1996
79. Hsu M, Savas U, Griffin K, Johnson E: Identification of peroxisome proliferators-responsive human genes by elevated expression of peroxisome proliferators-activated receptor α in HepG2 Cells. J. Biol. Chem 276:27950–27958, 2001
80. Neuschwander-Tetri BA, Brunt EM, Wehmeier KR, Oliver D, Bacon BR: Improved nonalcoholic steatohepatitis after 48 weeks of treatment with the PPAR-gamma ligand rosiglitazone. Hepatology 38:008–1017, 2003
81. Promrat K, Lutchman G, Uwaifo GI, Freedman RJ, Soza A, Heller T, Doo E, Ghany M, Premkumar A, Park Y, Liang TJ, Yanovski JA, Kleiner DE, Hoofnagle JH: A pilot study of pioglitazone treatment for nonalcoholic steatohepatitis. Hepatology 39:188–196, 2004

Digestive Diseases and Sciences, Vol. 50, No. 5 (May 2005), pp. 942–948 (© 2005)
DOI: 10.1007/s10620-005-2669-7

Angiotensin II Participates in Hepatic Inflammation and Fibrosis through MCP-1 Expression

KEISHI KANNO, MD,* SUSUMU TAZUMA, MD,† TOMOJI NISHIOKA, MD,* HIDEYUKI HYOGO, MD,† and KAZUAKI CHAYAMA, MD*

In this study, we assessed the hypothesis that angiotensin (Ang) II could modulate inflammatory cell recruitment into the liver through hepatic expression of monocyte chemoattractant protein (MCP)-1 during liver injury. For in vivo study, Ang II type 1a knockout (AT1a KO) mice and wild-type (WT) mice were treated with CCl_4 for 4 weeks. After CCl_4 treatment, AT1a KO mice showed lower expression of MCP-1 and fewer CD68-positive cells in the liver compared with WT mice. For in vitro study, Ang II was added to LI90 cells. Ang II enhanced MCP-1 mRNA together with RhoA mRNA and also induced secretion of MCP-1 into the culture medium. This change was strongly blocked by Y-27632, a specific Rho-kinase inhibitor. These results suggest that Ang II modulates hepatic inflammation via production of MCP-1 by hepatic stellate cells, and the effect of Ang II on MCP-1 production is, at least partly, mediated by the Rho/Rho-kinase pathway.

KEY WORDS: renin–angiotensin system; monocyte chemoattractant protein-1; hepatic stellate cell; hepatic inflammation; hepatic fibrosis; angiotensin II type 1a knockout mouse; small G protein; Rho/Rho-kinase pathway; carbon tetrachloride.

The renin–anigiotensin system (RAS) not only plays an important role in the regulation of systemic hemodynamics, but also functions as a growth factor in various organs, including the vasculature, kidneys, and liver. Activated hepatic stellate cells (HSCs), which are major producers of extracelluar matrix after liver injury, express the angiotensin (Ang) II receptor (1), and inhibition of Ang II synthesis or blockade of Ang II signaling reduces experimental hepatic fibrosis (2–4). Our previous study showed that mice lacking the Ang II type 1a receptor (AT1a) were resistant to the development of hepatic fibrosis after exposure to carbon tetrachloride (CCl_4) (5). Moreover, local hepatic expression of key components of the RAS was up-regulated in an animal model of bile duct ligation (6), and the major cellular source of Ang II in the fibrotic liver was shown to be HSC (7). Overall, these reports support a contribution of the RAS to hepatic fibrogenesis.

Chemokines are low molecular weight secretory proteins that principally stimulate leukocyte recruitment. There are four defined chemokine subfamilies based on their primary structure, CXC, CC, C, and CX_3C. Monocyte chemoattractant protein (MCP)-1, which belongs to the CC subfamily, regulates the recruitment and activation of inflammatory cells, including monocytes/macrophages and T lymphocytes (8, 9). These inflammatory cells that infiltrate into the liver promote the progression of hepatic fibrosis by releasing various mediators (10). In fact, MCP-1 expression is up-regulated in the livers of patients with active cirrohosis (11), and activated HSCs are predominantly responsible for MCP-1 production (12). MCP-1 is secreted by various types of cultured cells. Among them, rat vascular smooth muscle cells (VSMCs)

Manuscript received July 27, 2004; accepted September 28, 2004.
From the *Department of Medicine and Molecular Science, Graduate School of Biomedical Sciences, Hiroshima University, and †Division of General Medicine, Hiroshima University Medical Hospital, Hiroshima, Japan.
Address for reprint requests: Susumu Tazuma, MD, Division of General Medicine, Hiroshima University Medical Hospital, 1-2-3, Kasumi, Minami-ku, Hiroshima 734-8551, Japan; stazuma@hiroshima-u.ac.jp.

(13) and cardiac fibroblasts (14) are stimulated to produce MCP-1 by Ang II.

A small GTPase, Rho, is thought to trigger the intracellular pathways that lead to the activation of several transcription factors and nuclear signaling. Previous studies have detected RhoA in activated HSC, and Rho signaling pathways play a prominent role in the activation of HSCs (15, 16). Administration of Y-27632, a specific Rho-kinase inhibitor, has an inhibitory effect on the progression of experimental liver fibrosis in animal models (17, 18). Furthermore, Rho and Rho-kinase are involved in Ang II-induced expression of MCP-1 by VSMCs (13).

We hypothesized that Ang II may act on HSC to induce MCP-1 during liver injury, thereby modulating inflammatory cell infiltration and subsequent hepatic fibrosis. In addition, we examined the role of Rho/Rho-kinase in Ang II-mediated production of MCP-1 by LI90 cells, an HSC cell line.

MATERIALS AND METHODS

Animals. AT1a knockout (AT1a KO) mice were established and kindly provided by Dr. Sugaya (19). C57BL/6 mice were obtained from Hiroshima Jikken Doubutsu (Hiroshima, Japan). Both strains of mice had the same genetic background and animals 6–8 weeks old were used in this study. The mice were allowed free access to food and water and were housed at a constant temperature with a 12-hr light/dark cycle during the study period. Liver fibrosis was induced by the subcutaneous injection of CCl_4 (Wako Pure Chemical Industries, Osaka, Japan) at a dose of 1.0 ml/kg (1:1 in mineral oil) twice weekly for 4 weeks. Mice were killed and livers were harvested at 3 days after the last injection. All animal procedures were done according to our institutional guidelines.

Immunohistological Examination. Liver tissues were fixed in 4% paraformaldehyde, embedded in paraffin, and cut into 5-μm-thick sections. Immunohistochemical analysis was routinely performed using either a goat polyclonal antibody for MCP-1 (1:100 dilution; Santa Cruz Biotechnology, Santa Cruz, CA) or CD68 (1:50 dilution; Santa Cruz Biotechnology). Several fields per slide were randomly selected for examination, and representative results from three animals are shown.

Cell Culture. LI90 cells (JCRB0160), which were derived from human HSCs (20), were provided by the Japan Health Science Foundation (Tokyo). LI90 cells were grown to confluence in Dulbecco's modified Eagle's medium (DMEM; Sigma–Aldrich, Japan) containing 10% fetal bovine serum (FBS; Gibco, Invitrogen, Japan) in uncoated plastic dishes, and then growth arrest was achieved by culture in DMEM without FBS for 2 days before use in the experiments.

RT-PCR. The steady-state level of each messenger RNA (mRNA) was assessed by a semiquantitative polymerase chain reaction (PCR) using GAPDH or β-actin as the housekeeping gene. RNA was isolated with the RNeasy Mini-kit (Qiagen, Germany) according to the manufacturer's instructions. Then single-stranded complementary DNA (cDNA) was synthesized from 1 μg of RNA using 0.5 nmol of each random primer and subjected to PCR. Subsequently, the synthesized cDNA was amplified using specific sets of primers for mouse MCP-1 (forward, ATGCAGGTCCCTGTCATG; reverse, GCTTGAGGTGGTTGTGGA) (21), mouse GAPDH (forward, TGAAGGTCGGTGTGAACGGATTTGGC; reverse, CATGTAGGCCATGAGGTCCACC AC) (21), human MCP-1 (forward, GACCACCTGGACAAGCAAAC; reverse, CTCAAAACATCCCAGGGGTA) (22), human RhoA (forward, CTGGTGATTGTTGGTGATGG; reverse, GCGATCATAATCTTCCTGCC) (23), and human β-actin (forward, GAGCGGGAAATCGTGCGTGACATT; reverse, GATGGAGTTGAAGGTAGTTTCGTG) (22). The PCR procedure used has been described previously (21–23). An aliquot (10 μl) of each PCR product was loaded onto a 2% agarose gel and stained with ethidium bromide. Then the band intensities were analyzed by densitometry.

Quantification of MCP-1 Protein by ELISA. Culture medium of nonstimulated LI90 cells or LI90 cells stimulated with Ang II for 2 days was collected and centrifuged at 12,000 rpm for 1 min. The supernatant was stored at −80°C until assay. MCP-1 was measured using a commercial enzyme-linked immunosorbent assay kit (Chemicon International, USA) according to the manufacturer's instructions.

NF-κB Activity Assay. LI90 cells were stimulated with 10^{-7} *M* Ang II for 1 hr with or without pretreatment using Y-27632 (Calbiochem–Novabiochem, USA) at a concentration of 10^{-5} *M* for 30 min. Nuclear extracts were prepared with a Nuclear Extraction kit (Active Motif, Japan), and the protein content was standardized. Then NF-κB activity was measured in the nuclear extracts using an NF-κB P65 Transcription Factor Assay kit (Chemicon International) according to the manufacturer's instruction.

Statistical Analysis. Results are expressed as the mean ± SD. Statistical analysis was performed using one-way analysis of variance (ANOVA) and $P < 0.05$ was considered to indicate significance.

RESULTS

Hepatic MCP-1 Expression in CCl_4-Treated Mice. RT-PCR revealed the up-regulation of hepatic MCP-1 mRNA expression in CCl_4-treated WT mice, whereas it was negligible in CCl_4-treated and untreated AT1a KO mice (Figure 1). Immunohistochemical analysis also confirmed the enhanced hepatic expression of MCP-1 protein in CCl_4-treated WT mice. After CCl_4 treatment

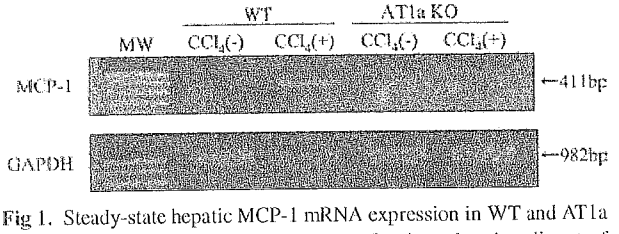

Fig 1. Steady-state hepatic MCP-1 mRNA expression in WT and AT1a KO mice with or without CCl_4 treatment for 4 weeks. An aliquot of each PCR product was loaded onto a 2% agarose gel and stained with ethidium bromide. Amplification of GAPDH was done to confirm the equal amounts of mRNA in each sample. The result shown here is representative of three independent experiments.

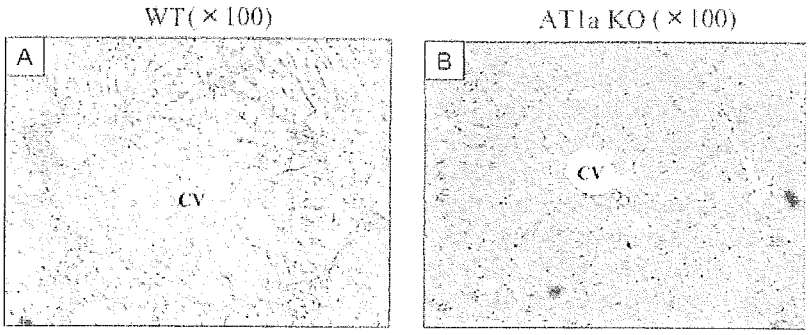

Fig 2. Immunohistochemical staining of MCP-1 in liver tissue from (A) a WT mouse and (B) an AT1A KO mouse after 4 weeks of CCl_4 treatment (1.0 ml/kg). CV, central vein. (Original magnification, ×100.)

for 4 weeks, MCP-1 staining was prominent in the portal tracts and fibrous septa of WT mice (Figure 2A). In contrast, the livers of CCl_4-treated AT1a KO mice showed almost no MCP-1 staining (Figure 2B) and were similar to the livers of the untreated groups (data not shown).

Hepatic CD68-Positive Cells in CCl_4-Treated Mice. As chemokines are considered to affect the recruitment of inflammatory cells, immunohistochemistry for the activated monocyte/macrophage marker CD68 (the main targets of MCP-1) was performed. In CCl_4-treated WT mice, the number of CD68-expressing cells was markedly increased in the portal tracts (Figure 3A). On the other hand, CCl_4 treatment had little influence on the number of CD68-expessing cells in the livers of AT1a KO mice (Figure 3B). These observations demonstrated that the number of CD68-expessing cells in the liver was associated with the expression of MCP-1.

Effect of Ang II on MCP-1 mRNA Expression. LI90 cells were stimulated with Ang II at a concentration of 10^{-7} *M*, and MCP-1 mRNA expression was examined at the indicated times by semiquantitative PCR. The expression of MCP-1 mRNA was enhanced, reaching a peak at 3 hr and returning to the basal level after 24 hr. The time course of MCP-1 mRNA expression was paralleled by the changes in RhoA mRNA (Figure 4A). Then LI90 cells were incubated with various concentrations of Ang II (10^{-11} to 10^{-5} *M*) for 3 hr. The expression of MCP-1 mRNA increased dose dependently and showed a pattern similar to that of RhoA mRNA (Figure 4B).

MCP-1 Protein Level in Culture Medium. To assess MCP-1 protein secretion into the culture medium, LI90 cells were stimulated with various concentrations of Ang II with or without Y-27632 pretreatment at a concentration of 10^{-5} *M*. Ang II dose dependently increased MCP-1 production after 48 hr of stimulation, and a significant difference was seen at a concentration of 10^{-7} or 10^{-5} *M*. Y-27632 markedly inhibited the secretion of MCP-1 protein induced by Ang II, whereas it had no suppressive effect on FBS-induced MCP-1 secretion (Figure 5).

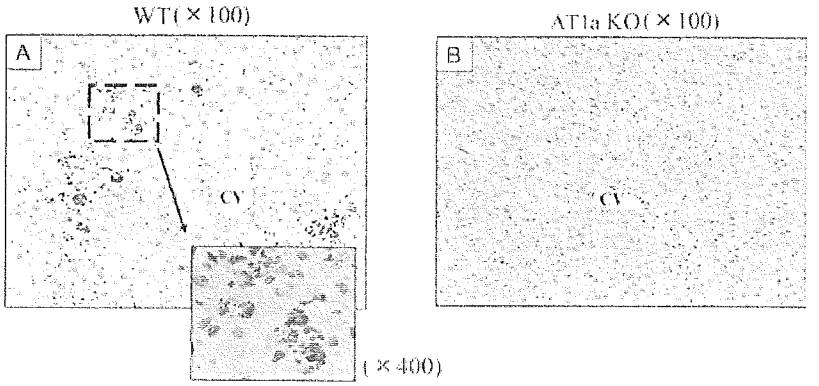

Fig 3. Distribution of CD68-positive cells in the liver. Immunohistocheical staining for CD68-positive mononuclear cells was performed in liver tissue from (A) a WT mouse and (B) an AT1A KO mouse after 4 weeks of CCl_4 treatment (1.0 ml/kg). CV, central vein. (Original magnification, ×100.)

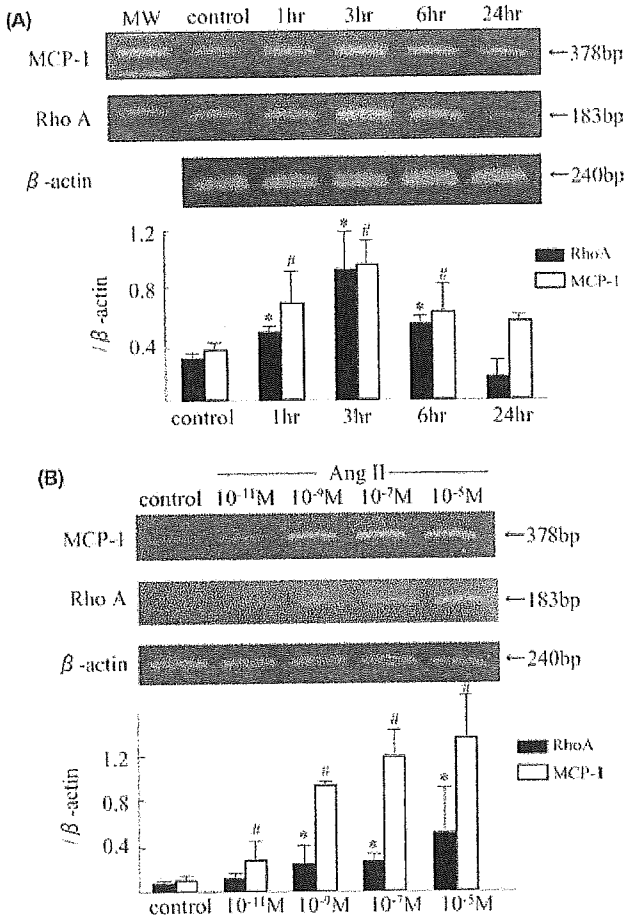

Fig 4. Effect of Ang II on MCP-1 mRNA expression by cultured LI90 cells. (A) Serum-starved LI90 cells were treated with 10^{-7} *M* Ang II at the indicated times, and the changes in Ang II-induced MCP-1 mRNA expression were examined by semiquantitative PCR. (B) Serum-starved LI90 cells were stimulated with Ang II at the indicated concentrations (10^{-11} to 10^{-5} *M*) for 3 hr, and MCP-1 mRNA expression was examined by semiquantitative PCR. Gels were scanned with a digital image analysis system, the products were quantified, and results are shown relative to the level of the housekeeping gene β-actin. Data from four independent experiments are shown as means ± SD. $^{*}P < 0.05$ vs. Rho A/β-actin of serum-free control; $^{\#}P < 0.05$ vs. MCP-1/β-actin of serum-free control.

Effect of Ang II on NF-κB Activity in LI90 Cells. NF-κB is the important factor involved in MCP-1 gene transcription in several cell types. To examine whether NF-κB participated in the induction of MCP-1 in Ang II-stimulated LI90 cells, NF-κB activity was studied. Growth-arrested LI90 cells were incubated with 10^{-7} *M* Ang II for 1 hr. In contrast to the up-regulation of MCP-1, Ang II did not activate NF-κB in LI90 cells (Figure 6).

DISCUSSION

There is accumulating evidence that the RAS is involved in hepatic fibrogenesis. Chronic liver injury up-regulates

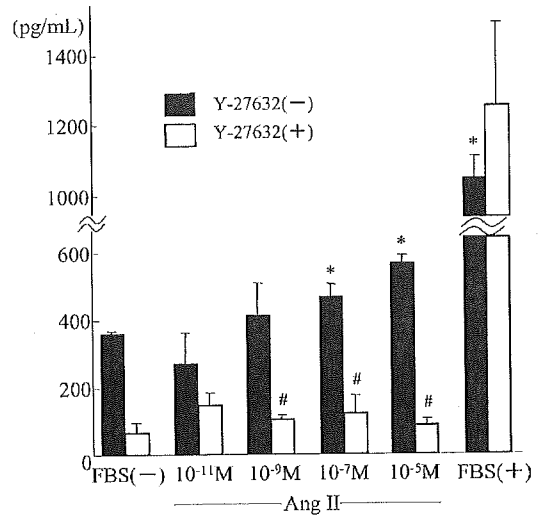

Fig 5. Effect of Ang II on MCP-1 secretion into the culture medium. Serum-starved LI90 cells were stimulated for 48 hr with the indicated concentrations of Ang II in the absence or presence of Y-27632 (10^{-5} *M*). Data from four independent experiments are shown as means ± SD. $^{*}P < 0.05$ vs. serum-free control. $^{\#}P < 0.05$ vs. each group without Y-27632.

key components of the RAS in an animal model of bile duct ligation (6), and RAS blockade ameliorates various types of experimental hepatic fibrosis (2–4). In patients with early chronic hepatitis C, an AT1 receptor antagonist decreased the area of hepatic fibrosis (24). We recently demonstrated that mice lacking the AT1 receptor are protected against CCl_4-induced hepatic fibrosis. Moreover, it was noteworthy that inflammatory infiltrates in the livers

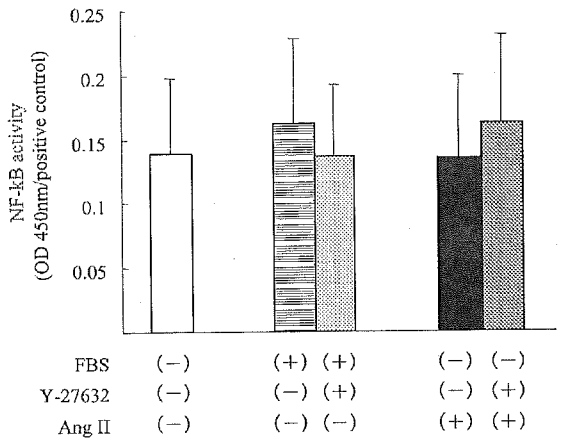

Fig 6. NF-κB activity in nuclear extracts of Ang II-stimulated LI90 cells. The cells were stimulated using Ang II for 1 hr with or without preincubation of Y-27632 (10^{-5} *M*). Then nuclear protein was extracted, and NF-κB activity was estimated. Absorbance values were standardized according to the protein concentration. The absorbance relative to that of the positive control (TNFα-stimulated whole Hela cells) from four independent experiments is shown as the mean ± SD.

of knockout mice were less severe compared with those in WT mice (5). This observation is in agreement with published data showing that prolonged systemic infusion of Ang II in normal rats induces hepatic inflammation (25). Therefore, there appears to be a close link between Ang II signaling and hepatic tissue inflammation.

MCP-1 is one of the potent chemokines that contributes to the accumulation of inflammatory cells. Since the recruitment of inflammatory cells depends on the expression of chemokines and adhesion molecules, hepatic MCP-1 expression is considered to play an important role in the pathogenesis of chronic hepatitis. MCP-1 levels have been reported to be elevated in the liver by treatment with CCl_4, endotoxin, or alcohol in experimental animals as well as in patients with chronic hepatitis (11, 12, 26, 27). In the present study, we demonstrated that mice lacking the AT1a receptor showed lower expression of MCP-1 and fewer CD68-positive cells in the liver after chronic CCl_4 treatment. These results do not mean the total elimination of hepatic inflammation but confirm that Ang II signaling via AT1a is critical for hepatic expression of MCP-1 and for the recruitment of mononuclear cells into the liver. According to the previous report (28), Kupffer cells play a critical role in the pathogenesis of hepatic inflammation and fibrosis through the release of biologically active mediators. In this regard, Ang II modulates hepatic inflammation via control of MCP-1 expression and subsequent mononuclear cells recruitment.

HSC can amplify inflammation through the release of chemokines such as MCP-1, and the up-regulation of such chemokines further amplifies inflammation during the process of liver injury (29, 30). In this study, we examined whether Ang II induces MCP-1 in cultured LI90 cells. Ang II enhanced the expression of MCP-1 mRNA together with RhoA mRNA in LI90 cells and, also, stimulated secretion of MCP-1 protein into the culture medium in a dose-dependent manner. Pharmacological blockade of Rho signaling with Y-27632, a specific inhibitor of Rho-kinase, strongly suppressed the Ang II-induced increase in MCP-1 production. The small G protein Rho is a member of the Rho family of small GTPases that also includes Rac and Cdc42. It is understood that Rho has a role in various cell functions, such as the control of cell morphology, proliferation, apoptosis, and regulation of various transcriptional factors. Recently, considerable attention has been paid to the role of Rho in the pathogenesis of hepatic fibrosis. Rho is reported to regulate the activation and proliferation of cultured HSC (15, 16), while administration of Y-27632 inhibits the development of hepatic fibrosis induced by dimethylnitrosamine (17) and CCl_4 (18) in animals. Furthermore, there are several lines of evidence for a close link between Ang II and the Rho signaling pathway. Ang II activates Rho in cultured VSMCs (13) and rat aortic endothelial cells (31), with induction of MCP-1 occurring in the former cell type. Interestingly, we found that Y-27632 did not suppress MCP-1 production when HSC were stimulated with FBS, which contains various growth factors. This suggests that the repressive effect of Y-27632 on MCP-1 production depends on the type of stimulation applied to HSC.

MCP-1 is produced by various types of cells, including HSC, monocytes, fibroblasts (14), and VSMCs (13), in response to a number of stimuli. Since the effects of different stimuli on MCP-1 expression are quite diverse among cell types, transcriptional activation generally seems to depend on an intricate series of regulatory mechanisms. Previous studies have indicated that NF-κB is the main factor involved in regulating the transcription

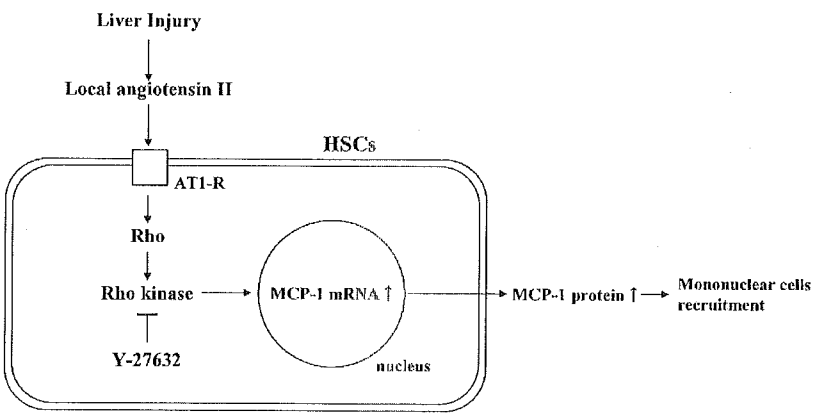

Fig 7. Speculated mechanism of how angiotensin II participates in hepatic inflammation after liver injury. Ang II enhances MCP-1 gene expression and synthesis, partly via the Rho signaling pathway, which modulate the recruitment of inflammatory cells into the liver. AT1-R, angiotensin II type1 receptor; HSCs, hepatic stellate cells.

of MCP-1 induced by LPS, IL-1β, TNF-α, and phorbal esters (32, 33). It was also reported that Ang II promotes MCP-1 expression via activation of NF-κB in cultured glomerular mesangial cells (34), as well as macrophages and VSMCs (13). Moreover, systemic Ang II infusion increases the DNA-binding activity of NF-κB in animals (25). Contrary to our expectation, the present study demonstrated that the level of NF-κB activity in LI90 cells was not altered by Ang II. However, this result is in agreement with the findings of a recent study using primary cultured human HSC (35), so further investigation is needed.

In conclusion, the present study demonstrated that the lack of Ang II signaling reduces the hepatic expression of MCP-1 and recruitment of activated Kupffer cells in a CCl_4-induced hepatic fibrosis model. In cultured LI90 cells, it was also shown that Ang II enhances MCP-1 gene expression and synthesis, partly via the Rho signaling pathway (Figure 7). These findings explain the mechanism by which inhibition of Ang II synthesis or blockade of AT1 signaling can reduce hepatic inflammation and subsequent fibrosis.

ACKNOWLEDGMENTS

This study was partly supported by a grant from the Japanese Ministry of Education, Culture, Sports, Science, and Technology to Dr. Tazuma (No. 12670489).

REFERENCES

1. Bataller R, Gines P, Nicolas JM, Gorbig MN, Garcia-Ramallo E, Gasull X, Bosch J, Arroyo V, Rodes J: Angiotensin II induces contraction and proliferation of human hepatic stellate cells. Gastroenterology 118:1149–1156, 2000
2. Wei HS, Li DG, Lu HM, Zhan YT, Wang ZR, Huang X, Zhang J, Cheng JL, Xu QF: Effects of AT1 receptor antagonist, losartan, on rat hepatic fibrosis induced by CCl 1(4). World J Gastroenterol 6:540–545, 2000
3. Jonsson JR, Clouston AD, Ando Y, Kelemen LI, Horn MJ, Adamson MD, Purdie DM, Powell EE: Angiotensin-converting enzyme inhibition attenuates the progression of rat hepatic fibrosis. Gastroenterology 121:148–155, 2001
4. Yoshiji H, Kuriyama S, Yoshii J, Ikenaka Y, Noguchi R, Nakatani T, Tsujinoue H, Fukui H: Angiotensin-II type 1 receptor interaction is a major regulator for liver fibrosis development in rats. Hepatology 34:745–750, 2001
5. Kanno K, Tazuma S, Chayama K: AT1A-deficient mice show less severe progression of liver fibrosis induced by CCl (4). Biochem Biophys Res Commun 308:177–183, 2003
6. Paizis G, Cooper ME, Schembri JM, Tikellis C, Burrell LM, Angus PW: Up-regulation of components of the renin-angiotensin system in the bile duct-ligated rat liver. Gastroenterology 123:1667–1676, 2002
7. Bataller R, Sancho-Bru P, Gines P, Lora JM, Al-Garawi A, Sole M, Colmenero J, Nicolas JM, Jimenez W, Weich N, Gutierrez-Ramos JC, Arroyo V, Rodes J: Activated human hepatic stellate cells express the renin-angiotensin system and synthesize angiotensin II. Gastroenterology 125:117–125, 2003
8. Loetscher P, Seitz M, Clark-Lewis I, Baggiolini M, Moser B: Monocyte chemotactic proteins MCP-1, MCP-2, and MCP-3 are major attractants for human CD4+ and CD8+ T lymphocytes. FASEB J 8:1055–1060, 1994
9. Gressner AM: Cytokines and cellular crosstalk involved in the activation of fat-storing cells. J Hepatol 22:28–36, 1995
10. Bernuau D, Rogier E, Feldmann G: In situ ultrastructural detection and quantitation of liver mononuclear phagocytes in contact with hepatocytes in chronic type B hepatitis. Lab Invest 51:667–674, 1984
11. Narumi S, Tominaga Y, Tamaru M, Shimai S, Okumura H, Nishioji K, Itoh Y, Okanoue T: Expression of IFN-inducible protein-10 in chronic hepatitis. J Immunol 158:5536–5544, 1997
12. Marra F, DeFranco R, Grappone C, Milani S, Pastacaldi S, Pinzani M, Romanelli RG, Laffi G, Gentilini P: Increased expression of monocyte chemotactic protein-1 during active hepatic fibrogenesis: correlation with monocyte infiltration. Am J Pathol 152:423–430, 1998
13. Funakoshi Y, Ichiki T, Shimokawa H, Egashira K, Takeda K, Kaibuchi K, Takeya M, Yoshimura T, Takeshita A: Rho-kinase mediates angiotensin II-induced monocyte chemoattractant protein-1 expression in rat vascular smooth muscle cells. Hypertension 38:100–104, 2001
14. Omura T, Yoshiyama M, Kim S, Matsumoto R, Nakamura Y, Izumi Y, Ichijo H, Sudo T, Akioka K, Iwao H, Takeuchi K, Yoshikawa J: Involvement of apoptosis signal-regulating kinase-1 on angiotensin II-induced monocyte chemoattractant protein-1 expression. Arterioscler Thromb Vasc Biol 24:270–275, 2004
15. Yee HF Jr: Rho directs activation-associated changes in rat hepatic stellate cell morphology via regulation of the actin cytoskeleton. Hepatology 28:843–850, 1998
16. Kato M, Iwamoto H, Higashi N, Sugimoto R, Uchimura K, Tada S, Sakai H, Nakamuta M, Nawata H: Role of Rho small GTP binding protein in the regulation of actin cytoskeleton in hepatic stellate cells. J Hepatol 31:91–99, 1999
17. Tada S, Iwamoto H, Nakamuta M, Sugimoto R, Enjoji M, Nakashima Y, Nawata H: A selective ROCK inhibitor, Y27632, prevents dimethylnitrosamine-induced hepatic fibrosis in rats. J Hepatol 34:529–536, 2001
18. Murata T, Arii S, Nakamura T, Mori A, Kaido T, Furuyama H, Furumoto K, Nakao T, Isobe N, Imamura M: Inhibitory effect of Y-27632, a ROCK inhibitor, on progression of rat liver fibrosis in association with inactivation of hepatic stellate cells. J Hepatol 35:474–481, 2001
19. Sugaya T, Nishimatsu S, Tanimoto K, Takimoto E, Yamagishi T, Imamura K, Goto S, Imaizumi K, Hisada Y, Otsuka A, Uchida H, Sugiura K, Fukuta K, Fukamizu A, Murakami K: Angiotensin II type 1a receptor-deficient mice with hypotension and hyperreninemia. J Biol Chem 270:18719–18722, 1995
20. Murakami K, Abe T, Miyazawa M, Yamaguchi M, Masuda T, Matsuura T, Nagamori S, Takeuchi K, Abe K, Kyogoku M: Establishment of a new human cell line, LI90, exhibiting characteristics of hepatic Ito (fat-storing) cells. Lab Invest 72:731–739, 1995
21. Ousman SS, David S: MIP-1 alpha, MCP-1, GM-CSF, and TNF-alpha control the immune cell response that mediates rapid phagocytosis of myelin from the adult mouse spinal cord. J Neurosci 21:4649–4656, 2001

22. Von Bubnoff D, Matz H, Cazenave JP, Hanau D, Bieber T, De La Salle H: Kinetics of gene induction after Fc epsilon RI ligation of atopic monocytes identified by suppression subtractive hybridization. J Immunol 169:6170–6177, 2002
23. Kamai T, Arai K, Tsujii T, Honda M, Yoshida K: Overexpression of RhoA mRNA is associated with advanced stage in testicular germ cell tumour. BJU Int 87:227–231, 2001
24. Terui Y, Saito T, Watanabe H, Togashi H, Kawata S, Kamada Y, Sakuta S: Effect of angiotensin receptor antagonist on liver fibrosis in early stages of chronic hepatitis C. Hepatology 36:1022, 2002
25. Bataller R, Gabele E, Schoonhoven R, Morris T, Lehnert M, Yang L, Brenner DA, Rippe RA: Prolonged infusion of angiotensin II into normal rats induces stellate cell activation and proinflammatory events in liver. Am J Physiol Gastrointest Liver Physiol 285:G642–G651, 2003
26. Czaja MJ, Geerts A, Xu J, Schmiedeberg P, Ju Y: Monocyte chemoattractant protein 1 (MCP-1) expression occurs in toxic rat liver injury and human liver disease. J Leukoc Biol 55:120–126, 1994
27. Afford SC, Fisher NC, Neil DA, Fear J, Brun P, Hubscher SG, Adams DH: Distinct patterns of chemokine expression are associated with leukocyte recruitment in alcoholic hepatitis and alcoholic cirrhosis. J Pathol 186:82–89, 1998
28. Luckey SW, Petersen DR: Activation of Kupffer cells during the course of carbon tetrachloride-induced liver injury and fibrosis in rats. Exp Mol Pathol 71:226–240, 2001
29. Phillips MI, Kagiyama S: Angiotensin II as a pro-inflammatory mediator. Curr Opin Investig Drugs 3:569–577, 2002
30. Pinzani M, Marra F: Cytokine receptors and signaling in hepatic stellate cells. Semin Liver Dis 21:397–416, 2001
31. Kunieda Y, Nakagawa K, Nishimura H, Kato H, Ukimura N, Yano S, Kawano H, Kimura S, Nakagawa M, Tsuji H: HMG CoA reductase inhibitor suppresses the expression of tissue factor and plasminogen activator inhibitor-1 induced by angiotensin II in cultured rat aortic endothelial cells. Thromb Res 110:227–234, 2003
32. Ueda A, Okuda K, Ohno S, Shirai A, Igarashi T, Matsunaga K, Fukushima J, Kawamoto S, Ishigatsubo Y, Okubo T: NF-kappa B and Sp1 regulate transcription of the human monocyte chemoattractant protein-1 gene. J Immunol 153:2052–2063, 1994
33. Hernandez-Presa M, Bustos C, Ortego M, Tunon J, Renedo G, Ruiz-Ortega M, Egido J: Angiotensin-converting enzyme inhibition prevents arterial nuclear factor-kappa B activation, monocyte chemoattractant protein-1 expression, and macrophage infiltration in a rabbit model of early accelerated atherosclerosis. Circulation 95:1532–1541, 1997
34. Ruiz-Ortega M, Bustos C, Hernandez-Presa MA, Lorenzo O, Plaza JJ, Egido J: Angiotensin II participates in mononuclear cell recruitment in experimental immune complex nephritis through nuclear factor-kappa B activation and monocyte chemoattractant protein-1 synthesis. J Immunol 161:430–439, 1998
35. Bataller R, Schwabe RF, Choi YH, Yang L, Paik YH, Lindquist J, Qian T, Schoonhoven R, Hagedorn CH, Lemasters JJ, Brenner DA: NADPH oxidase signal transduces angiotensin II in hepatic stellate cells and is critical in hepatic fibrosis. J Clin Invest 112:1383–1394, 2003

GASTROENTEROLOGY 2005;128:138–146

Suppression of Macrophage Infiltration Inhibits Activation of Hepatic Stellate Cells and Liver Fibrogenesis in Rats

MICHIO IMAMURA,*,† TADASHI OGAWA,* YASUYUKI SASAGURI,§ KAZUAKI CHAYAMA,† and HIKARU UENO*

*Department of Biochemistry and Molecular Pathophysiology, University of Occupational and Environmental Health, School of Medicine, Kitakyushu, Japan; †Department of Medicine and Molecular Science, Graduate School of Biomedical Science, Hiroshima University, Hiroshima, Japan; and §Department of Pathology and Cell Biology, University of Occupational and Environmental Health, School of Medicine, Kitakyushu, Japan

Background & Aims: Monocytes/macrophages infiltrate into injured livers. We tried to clarify their roles in inflammation and subsequent fibrogenesis by inhibiting their infiltration with a mutated form (7ND; 7 amino acids at the N-terminal were deleted) of monocyte chemoattractant protein 1, which may function as a dominant-negative mutant. *Methods:* Rats were injected via the tail vein with an adenovirus expressing either human 7ND (Ad7ND), a truncated type II transforming growth factor β receptor (AdTβ-TR), which works as a dominant-negative receptor, bacterial β-galactosidase (AdLacZ), or saline. Seven days later, the rats were treated with dimethylnitrosamine for 1–21 days. *Results:* Within 24 hours after a single dimethylnitrosamine injection, macrophages were observed in livers. With a 3-day dimethylnitrosamine treatment, activated hepatic stellate cells were detectable in livers in AdLacZ-, AdTβ-TR–, and saline-injected rats. In contrast, in the Ad7ND-treated rats, infiltration of macrophages was markedly reduced, and activated hepatic stellate cells were not detectable. After a 3-week dimethylnitrosamine treatment, fibrogenesis was almost completely inhibited, and activated hepatic stellate cells were hardly seen in livers in both Ad7ND- and AdTβ-TR–treated rats. *Conclusions:* Our results show that blockade of macrophage infiltration inhibits activation of hepatic stellate cells and leads to suppression of liver fibrogenesis. The presence of activated hepatic stellate cells in the initial phase after injury and its absence at a later phase in the AdTβ-TR–treated livers indicate that transforming growth factor β is not an activating factor for hepatic stellate cells, and this suggests that transforming growth factor β is required for the survival of activated hepatic stellate cells. Our study suggests that infiltrated macrophages may themselves produce an activating factor for hepatic stellate cells.

Inflammation is always accompanied by an infiltration by leukocytes,[1] a process that is thought to be regulated by chemotactic cytokines called *chemokines*.[1,2] Monocyte chemoattractant protein (MCP)-1, one of these chemokines, induces infiltration by monocytes/macrophages and lymphocytes[3] by binding to a specific receptor, CCR2.[1,2] In animal models of liver injury[4,5] and in patients with chronic hepatitis,[6,7] MCP-1 is detectable in both livers and serum. Injury-induced inflammation results in tissue remodeling or liver fibrosis. However, the actual roles performed by infiltrated monocytes/macrophages and MCP-1 in liver fibrogenesis are largely unknown.

During liver fibrogenesis, hepatic stellate cells (HSC) are activated to myofibroblast-like cells expressing α-actin. These activated HSC and myofibroblasts already existing in the portal field and around central veins may play a central role in fibrogenesis,[8] after which they produce extracellular matrix through the generation of various cytokines, including transforming growth factor (TGF)-β.[9] For fibrogenesis, HSC are considered to be the responsible cells, and TGF-β is one of the critical factors for fibrogenesis. In fact, when we inhibited the action of TGF-β by using a dominant-negative mutated receptor for TGF-β,[10] the activated HSC were markedly reduced in number, and fibrogenesis, as well as the progression of already-established fibrosis, was almost completely suppressed.[11–13] This shows the essential roles played by TGF-β and HSC in fibrotic remodeling after liver injury. However, the mechanism underlying the activation of HSC is not fully understood, although TGF-β has been believed to be an activating factor.[14]

In this study, to try to answer these questions, we introduced a mutated form of MCP-1 (7ND), which is

Abbreviations used in this paper: DMN, dimethylnitrosamine; ELISA, enzyme-linked immunosorbent assay; HSC, hepatic stellate cells; MCP, monocyte chemoattractant protein; MOI, multiplicity of infection; TGF, transforming growth factor; TUNEL, terminal deoxynucleotidyl transferase–mediated deoxyuridine triphosphate nick-end labeling.

0016-5085/05/$30.00
doi:10.1053/j.gastro.2004.10.005

considered to inhibit the action of MCP-1 as a dominant-negative mutant,[15,16] into dimethylnitrosamine (DMN)-treated rats, an established model of liver fibrosis with a pathology closely resembling that of human cirrhosis.[17,18] Some rats were given a dominant-negative TGF-β receptor to eliminate signaling by TGF-β.[11,12] We compared these rats in terms of (1) infiltration by monocytes/macrophages and activation of HSC, both of which occur in the acute phase after injury, and (2) fibrotic changes in the chronic phase after injury. Although inhibition of MCP-1 and blockade of TGF-β each led to a marked suppression of liver fibrogenesis, we were interested to find that some responses in the initial phase after injury were quite different between these 2 groups. Our study indicates that TGF-β is not an activating factor for HSC and suggests that infiltrated monocytes/macrophages may produce the activating factor(s).

Materials and Methods

Preparation of Adenoviruses

Replication-defective E1$^-$ and E3$^-$ adenoviral vectors expressing an amino-terminal deletion mutant of human MCP-1 (Ad7ND) with a FLAG epitope tag in its carboxyl-terminal (complementary DNA, a generous gift from Dr. B. Rollins, Harvard University),[15,16] a truncated human TGF-β type II receptor (AdTβ-TR),[10–12] or bacterial β-galactosidase (AdLacZ)[19] under a CA promoter comprising a cytomegalovirus enhancer and a chicken β-actin promoter[20] were prepared as previously described.[21]

Detection of Mutated Human Monocyte Chemoattractant Protein 1 (7ND) and Rat Wild-Type Monocyte Chemoattractant Protein 1

COS cells were infected with either Ad7ND (multiplicity of infection [MOI] of 1, 10, and 100) or AdLacZ (MOI of 10), as previously described.[10] One day after infection, the medium was replaced with serum-free medium, and cells were incubated for a further 24 hours. A mutant MCP-1 (7ND) secreted into culture media was analyzed by Western blotting by using monoclonal antibodies against either FLAG (Abcam, Cambridge, UK) or human MCP-1 (Sanbio, 5400 AM Uden, The Netherlands), as previously described.[13]

7ND and rat MCP-1 were also detectable by enzyme-linked immunosorbent assay (ELISA). Livers were homogenized in phosphate-buffered saline with 1% Triton X-100, 0.1% sodium dodecyl sulfate, and 0.5% sodium deoxycholate. The homogenates were centrifuged at 20,000*g* for 30 minutes. 7ND and rat MCP-1 were measured in the supernatant of liver homogenates and in sera from rats by using a human MCP-1 ELISA kit (Biosource, Camarillo, CA) and a rat kit (Biosource), respectively, according to the manufacturer's instructions. These ELISA kits are species specific, and cross-reaction between human and rat MCP-1 is less than 5%. In fact, no human MCP-1 protein was detectable in samples from either intact or AdLacZ-infected rats (data not shown).

Animal Models

All animals were treated under protocols approved by the institutional animal care committees, and the experiment was performed under both the institutional guidelines for animal experiments and by the Law (No. 105) and Notification (No. 6) of the Japanese government. Male Sprague–Dawley rats, 10 weeks old and weighing approximately 350 g, were given a single infusion of 0.5 mL of Ad7ND, AdTβ-TR, AdLacZ (2×10^9 plaque-forming units per milliliter), or saline via the tail vein, as previously reported.[12] By this method, virtually all cells in the liver were infected and expressed the introduced molecule.[11,12] Seven days later, rats were given an intraperitoneal injection of DMN (10 μg/g body weight; Wako, Osaka, Japan) either once or at the indicated times (3 consecutive daily injections or 3 consecutive daily injections and 4 days off per week for 3 weeks), as previously reported.[11–13] After DMN treatment, blood was collected, and the rats were killed. Biochemical parameters were measured by using standard methods. The liver was either fixed with 4% buffered paraformaldehyde for histological examination or frozen immediately in liquid nitrogen for the extraction of hydroxyproline, the content of which was measured as described elsewhere.[22]

Histological Examination

Liver sections were stained with hematoxylin or Masson trichrome or subjected to immunohistostaining by using antibodies against either CD68 (ED-1; Serotec, Raleigh, NC) or α-actin (Dako, Tokyo, Japan). Immunoreactive materials were visualized by using a streptavidin-biotin staining kit (Histofine SAB-PO kit; Nichirei, Tokyo, Japan) and diaminobenzidine. Macrophages (CD68-positive cells) and lymphocytes were counted by a technician blinded to the treatment regimen. Four random high-power (200×) fields from each section were examined. As negative controls, immunohistostaining was performed without the first antibodies.

Determination of Hepatic Stellate Cells in Apoptosis

Fragmented DNA in apoptotic cells in liver sections was stained with diaminobenzidine (dark brown) by the terminal deoxynucleotidyl transferase–mediated deoxyuridine triphosphate nick-end labeling (TUNEL) technique by using a commercially available kit (Roche Diagnostics, Mannheim, Germany). Then, the sections were double-stained against α-actin and visualized with the aid of 3-amino-9-ethyl carbazole liquid substrate chromogen (red; Dako). As negative controls, the TUNEL reaction mixture was used without terminal transferase.

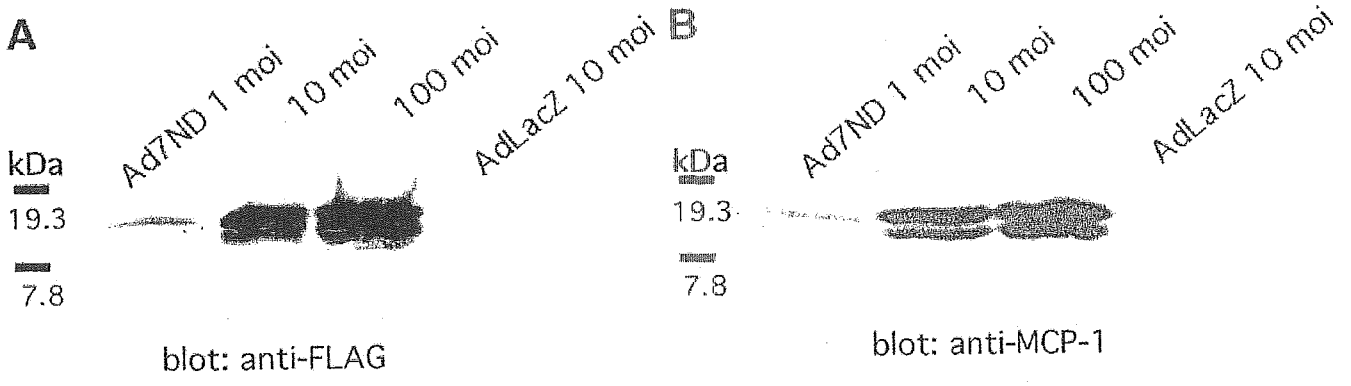

Figure 1. A mutated form of MCP-1 (7ND) is secreted from cells infected with Ad7ND. COS cells were infected either with Ad7ND or with AdLacZ at the indicated MOI. After 48 hours, the culture media were subjected to sodium dodecyl sulfate-polyacrylamide gel electrophoresis (12%) and analyzed by Western blotting by using antibodies against either (*A*) FLAG or (*B*) human MCP-1. Molecular markers are in kilodaltons.

Statistical Analysis

Statistical analysis was performed by 1-way analysis of variance followed by Scheffé's test. $P < .05$ was considered significant.

Results

A Mutant Monocyte Chemoattractant Protein 1, 7ND, Was Secreted From Ad7ND-Infected Cells and Detected in the Serum and Liver of Ad7ND-Infected Rats

In the culture medium from Ad7ND-infected COS cells, 7ND was readily detectable in an MOI-dependent manner, as assessed by Western blotting analysis (Figure 1). Human 7ND and endogenous rat MCP-1 proteins were measured in sera (Figure 2*A*) and liver extracts (Figure 2*B*) from rats infected with Ad7ND. Seven days after gene transfer, a 3-week DMN treatment was begun. It is interesting to note that the amount of rat MCP-1 was not significantly changed by DMN treatment in either serum or liver. 7ND reached a peak on the seventh day after gene transfer and then declined gradually; however, the values were much higher than those obtained for rat MCP-1 in most time periods under DMN injury.

Dimethylnitrosamine-Induced Infiltration by Macrophages and Lymphocytes and Activation of Hepatic Stellate Cells Were Both Suppressed in Ad7ND-Treated Livers

Rats were infused via the tail vein with either saline or an adenovirus expressing 1 of the following:

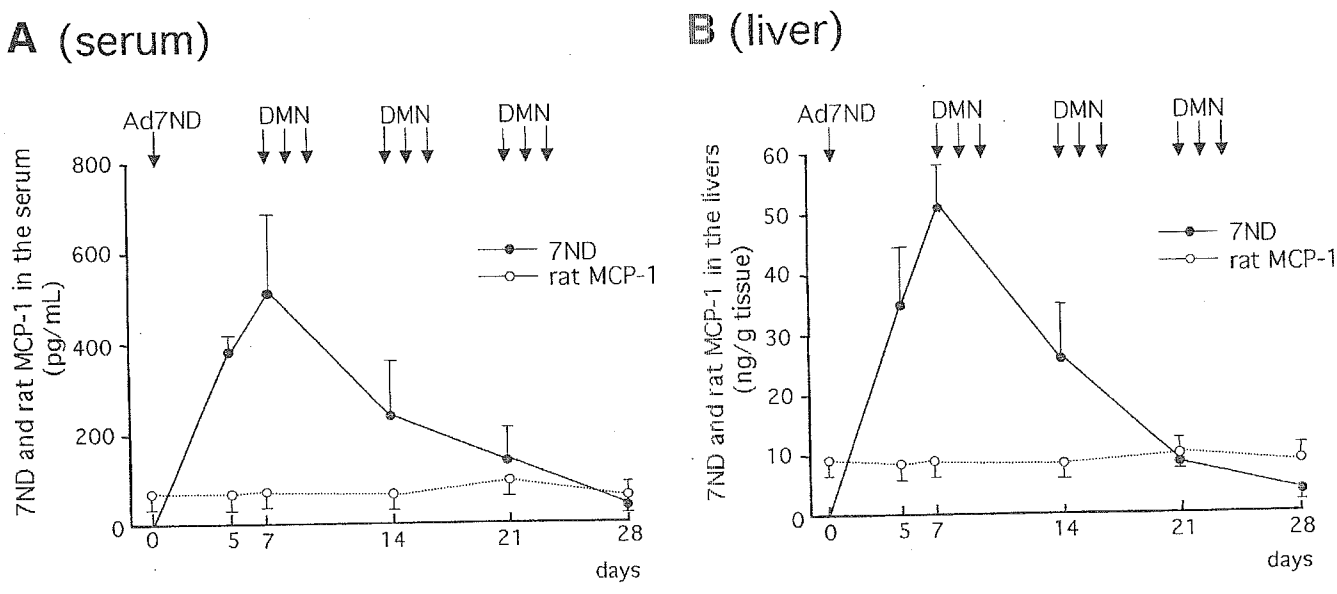

Figure 2. Amounts of human 7ND and rat MCP-1 in the sera (*A*) and livers (*B*) of DMN-injured rats. Rats were given a single infusion of Ad7ND (or saline infusion) via the tail vein. Seven days later, rats were subjected to a 3-week DMN treatment (shown as arrows). Rats were killed 5, 7 (just before the initiation of DMN treatment), 14, 21, and 28 days after Ad7ND injection. Means ± SD (n = 4) are shown.

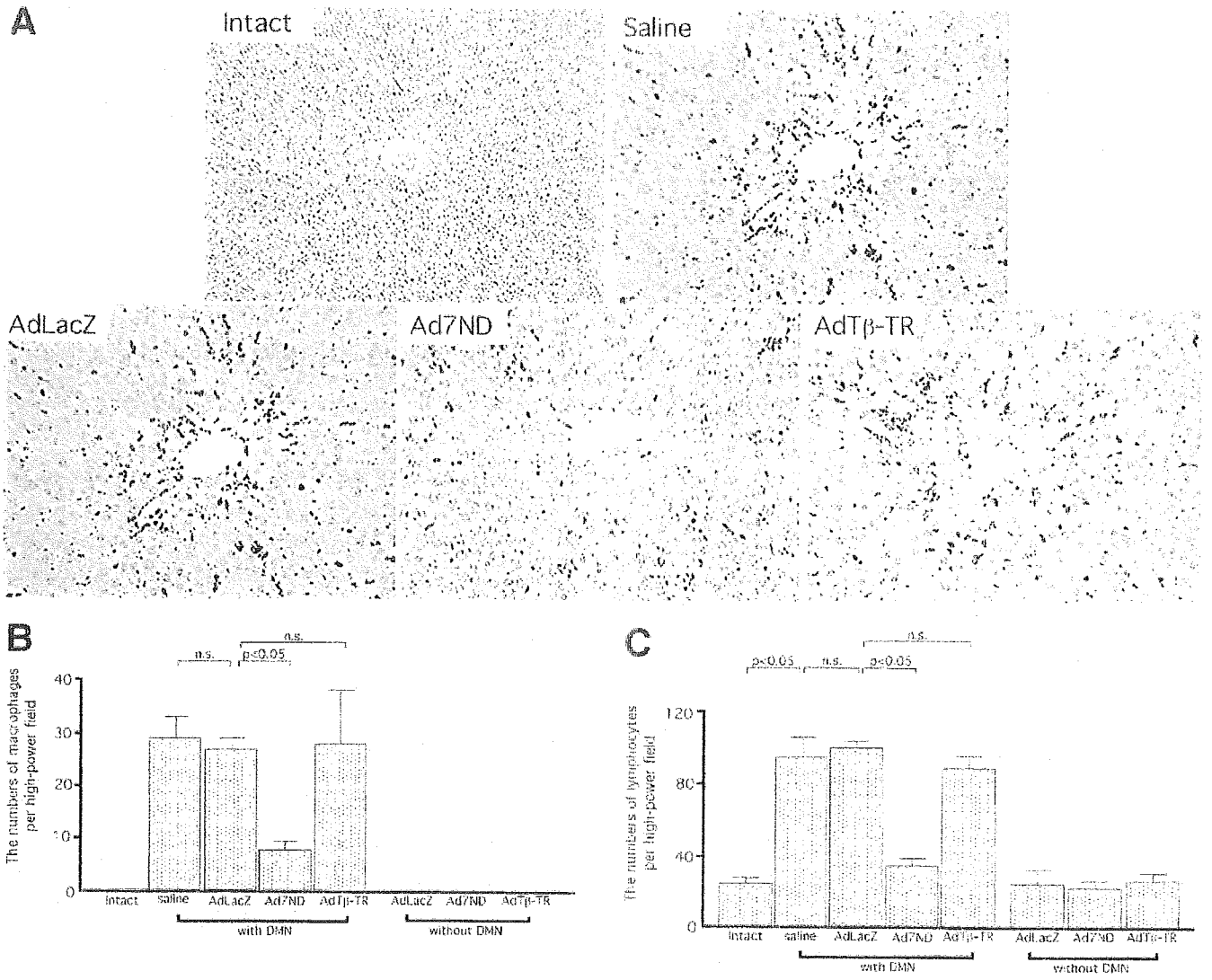

Figure 3. Infiltration of macrophages and lymphocytes into DMN-treated livers. Rats were given a single infusion of saline, AdLacZ, Ad7ND, or AdTβ-TR via the tail vein. Seven days later, some rats were administered DMN once (shown as *with DMN*) and some rats were not administered DMN (shown as *without DMN*; histology not shown). Twenty-four hours after the DMN challenge, they were killed, and liver sections were histologically examined either by immunohistostaining against CD68, to detect macrophages (*A*), or by hematoxylin staining for lymphocytes (not shown; original magnification, 200×). Similar histology was seen in all 4 rats in each group. The numbers of (*B*) macrophages and (*C*) lymphocytes were semiquantitated (see Materials and Methods). Four fields in each of 4 rats (a total of 16 fields in each group) were examined, and the number of cells per high-power field is shown as mean ± SD. n.s., statistically not significant. Rats never treated with adenovirus or DMN were also analyzed (shown as *intact*).

β-galactosidase (AdLacZ), a truncated TGF-β receptor (AdTβ-TR), or a mutated MCP-1 (Ad7ND). Seven days later (when the expression of the introduced molecules had reached a submaximal level), DMN was given. One day after a single injection of DMN, we analyzed liver sections by hematoxylin staining and immunohistostaining against CD68, which is a specific marker for macrophages. Macrophages were detectable in the centrilobular area of the livers of AdLacZ-infected, AdTβ-TR–infected, or saline-injected rats: there were no differences among these 3 groups. However, macrophages were greatly reduced in Ad7ND-treated livers (Figure 3*A*). The numbers of CD68-positive cells (per high-power field) were 29 ± 3.5 in saline-treated livers, 27.5 ± 2.1 in AdLacZ-treated livers, 27.5 ± 11.4 in AdTβ-TR–treated livers, and only 7.1 ± 1.2 in Ad7ND-treated livers (Figure 3*B*). Similarly, the numbers of lymphocytes (histology not shown) were 98 ± 7.5 in saline-treated livers, 101 ± 2.5 in AdLacZ-treated livers, 93 ± 5.5 in AdTβ-TR–treated livers, and only 40 ± 3.5 per high-power field in Ad7ND-treated livers (Figure 3*C*). Without DMN treatment, neither macrophages nor lymphocytes (histology not shown) were increased in the livers of AdLacZ-infected, AdTβ-TR–infected, and